REACTIONS OF OXOMOLYBDENUM COMPOUNDS WITH NITROGEN DONOR LIGANDS AND RELATED COMPUTATIONAL CALCULATIONS

A Thesis Submitted to
the Graduate School of Engineering and Science of
İzmir Institute of Technology
in Partial Fulfillment of the Requirements for the Degree of

MASTER OF SCIENCE

in Chemistry

by
Jale ÖCAL

September 2009
İZMİR

We approve the thesis of **Jale ÖCAL**

Prof. Işıl TOPALOĞLU-SÖZÜER
Supervisor

Assist. Prof. Armağan KINAL
Committee Member

Assist. Prof. Gülşah ŞANLI
Committee Member

04 September 2009

Prof. Levent ARTOK
Head of the Department of Chemistry

Assoc. Prof. Talat YALÇIN
Dean of the Graduate School of
Engineering and Sciences

ACKNOWLEDGEMENTS

Firstly, I want to thank my supervisor Prof. Işıl Topaloğlu Sözüer for her invaluable support during my thesis study. Secondly, I would thank to Assist. Prof. Armağan Kınal for his excellent guidance for all the computational calculations in his laboratory at Ege University. I also would like Assist. Prof. Nursel Acar Selçuki who encouraged me to begin to computational studies. Also, I would like to thank to the Research Foundation of Izmir Institute of Technology for financial support, Ege University for NMR analyses, Dr. Hüseyin Özgener for FT-IR spectra and elemental analyses. I am also very thankful to my lab mates and friends at IYTE.

My special thanks go to the Organization of Turkish Education (TEV) for providing scholarship throughout my thesis. Being a member of the family TEV was a great honour for me.

Finally, I want to thank to my parents and my lovely sisters (N., S., E., Y., A.) and brother (O.) for their love, motivation, supports and affection.

ABSTRACT

REACTIONS OF OXOMOLYBDENUM COMPOUNDS WITH NITROGEN DONOR LIGANDS AND RELATED COMPUTATIONAL CALCULATIONS

Reactions of the dioxomolybdenum(VI) compound, $MoCl_2O_2$ with phenylenediamine derivatives the bidentate N-N nitrogen ligands **1-8** (o-phenylenediamine, N-phenyl-o-phenylenediamine, 4-Methyl-o-phenylenediamine, 4-Nitro-o-phenylenediamine, p-phenylenediamine, N-phenyl-p-phenylenediamine, 2,6-dichloro-p-phenylenediamine, 2,3,5,6-tetramethyl-p-phenylenediamine, respectively) have been examined under nitrogen in THF solution.

The novel dioxomolybdenum complexes were characterized by elemental analysis, FT-IR, ^{1}H-NMR and ^{13}C-NMR spectroscopy. In addition, molecular mechanics and quantum chemical calculations including semi empirical PM3 and DFT methods were carried out to discuss the stability of the compounds.

ÖZET

OKSOMOLİBDEN BİLEŞİKLERİNİN AZOT VERİCİSİ LİGANDLARLA REAKSİYONLARI VE İLGİLİ TEORİK HESAPLAMALAR

Dioksomolibden(VI) bileşiği, MoO_2Cl_2 ile çift dişli azot vericisi N-N ligandları olan fenilendiamin türevlerinin **1-8** (sırasıyla, o-fenilendiamin, N-fenil-o-fenilendiamin, 4-Metil-o-fenilendiamin, 4-Nitro-o-fenilendiamin, p-fenilendiamin, N-fenil-p-fenilendiamin, 2,6-dikloro-p-fenilendiamin, 2,3,5,6-tetrametil-p- fenilendiamin) reaksiyonları THF çözeltisinde azot altında yapıldı.

Yeni dioksomolibden complexlerinin karakterizasyonu elemental analiz, FT-IR, ^{1}H-NMR ve ^{13}C-NMR spektroskopisi ile yapıldı. Buna ilave olarak, bileşiklerin kararlılığını açıklamak için semi ampirik PM3 ve DFT metotlarını içeren moleküler mekanik ve kuantum kimyasal hesapları yapıldı.

TABLE OF CONTENTS

LIST OF FIGURES

LIST OF TABLES

CHAPTER 1

INTRODUCTION

1.1. Oxomolybdenum Chemistry

Molybdenum is considered as a trace element, presents several oxidation states, and therefore may change easily its coordination number and to form mono and binuclear oxo complexes which is of great importance from basic as well as applied points of view. The propensity of oxomolybdenum species in higher oxidation states to form di, tri and polynuclear complexes is well known (Garner, et al. 1987). Molybdenum is a relevant element for the synthesis of many homogeneous and heteregenous catalysts. The element is also essential in several enzymatic systems. One of the characteristics of the molybdenum chemistry is related to the easy conversion between its oxidation states and to the changes of coordination number, observed particularly between Mo(III), Mo(IV), Mo(V) and Mo(VI) (Garner, et al. 1995). Moreover among the oxidation states of Mo, 6+ is stabilized through formation of the MoO_2^{2+} (Chowdhury, et al. 2006).

The chemistry of dioxomolybdenum(VI) complexes is of importance especially in industrial and biochemical catalysis (Sellmann, et al. 1995). The coordination chemistry of molybdenum(VI) has attracted considerable interest due to its biological importance (Enemark, et al. 2004, Holm, et al. 1996) as well as for the importance of molybdenum(VI) complexes as catalysts in various oxidations reactions (Bäckvall 2004, Meunier 2000) , such as epoxidation and hydroxylation of olefines (Bregeault 2003, Jorgensen 1989, Rao, et al. 2000, Brito, et al. 2004) oxidation of alcohols (Lorber, et al. 2000) and as catalysts of oxygen atom transfer reactions (Holm, et al. 1990, Dinda, et al. 2002). Moreover, molybdate can catalyze the oxidation of bromide (Meister, et al. 1994) and some peroxo complexes of molybdenum(VI) have been found to oxidize bromide in a stoichiometric reaction (Reynolds, et al. 1997). Molybdenum(VI) chemistry often involves oxo chemistry, that is complexes that have an O^{2-} (oxo) ligand. Octahedral transition metal complexes containing two oxo ligands bonded to the metal can have two orientations, cis-dioxo or trans-dioxo. In general, transition metals having the d^0 electron

configuration contain two oxo groups in the cis orientation (at 90 degrees to each other in an octrahedral complex). Transition metals having the d^2 electron configuration generally contain two oxo groups in the trans orientation (at 180 degrees to each other in an octahedral complex). These two arrangements are illustrated below.

cis-dioxo trans-dioxo

Figure 1.1. Molybdenum containing oxo groups in the cis and trans orientation. (Source: Jurisson 1997)

Molybdenum(VI) has a d^0 electron configuration so its dioxo complexes usually have a cis-dioxo geometry. Tetrahedral geometries are also known for dioxo complexes. In this geometry there is no cis or trans.

Dichlorodioxomolybdenum(VI), MoO_2Cl_2, is a useful starting material for preparing a variety of molybdenum compounds. This Mo(VI) compound is tetrahedral in its arrangement of ligands around the molybdenum center. However, MoO_2Cl_2 is moisture sensitive (reacts with water to decompose) and must be prepared just before using it by chlorinating molybdenum(IV) oxide (MoO_2). A related, yet moisture stable molybdenum(VI) compound that is readily prepared and useful as a starting material for preparing a variety of Mo compounds in oxidation state VI as well as lower oxidation states (Jurisson 1997).

1.2. Catalytic Applications of Oxomolybdenum Complexes

Oxomolybdenum complexes are well known oxidation catalysts in chemistry. In particular Mo(VI) derivatives, such as MoO_2X_2 and WO_2X_2, give rise to molecules of formula $MO_2X_2(L–L)$ (M = Mo, W) in the presence of Lewis bases or even donor solvents (THF, NCH_3), which exhibit catalytic activity in olefin epoxidation reactions (Veiros, et al. 2006).

1.2.1. Solvent-Stabilized Oxomolybdenum Complexes

Oxomolybdenum complexes with the cis- MoO_2 fragment of the general formula $MoBr_2O_2(Solv)_2$ are very important precursors or oxidation catalysts, in chemical and in biological systems (Kumar, et al. 1991, Palanca, et al. 1990, Wilshire, et al. 1979). As starting material for synthesis of oxomolybdenum species with various nitrogen and oxygen donor ligands, it is prepared the complexes of the type $MoX_2O_2(Solv)_2$ (X = Cl, Br; (Solv) = THF, NCH_3) (Kühn, et al. 1999) The synthesis of compounds of general formula MoX_2O_2 $(Solv)_2$ is achieved by dissolving the molybdenumdioxo dichloride or bromide in donor solvent. The product complexes are nearly insoluble in nonpolar nondonor solvents (alkanes or diethyl ether) but are very soluble in most donor solvents (Gonçalves, et al. 2001). These complexes catalyze the epoxidation of olefins with t-butylhydroperoxide. They do not proceed significantly further in the catalytic run. The reason for that observation is the pronounced water sensitivity of the solvent-stabilized complexes. In contrast to other more strongly coordinating organic ligands, these compounds do not prevent the moisture-induced decomposition of the complexes. The $MoX_2O_2(Solv)_2$ complexes are therefore more useful as synthetic precursors for complexes with other, more strongly coordinating ligands than as catalysts themselves.

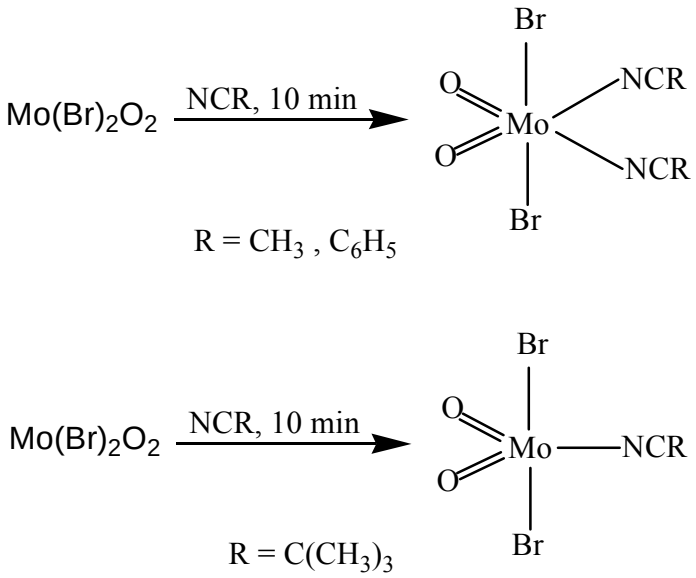

Figure 1.2. The synthesis of Solvent-Stabilized Oxomolybdenum Complexes (Source: Kühn, et al. 1999)

The complex $MoCl_2O_2(Solv)_2$ is very electron deficient and readily reacts with electron donor L-L N-ligands to give more stable complexes. (Gonçalves, et al. 2001)

1.2.2. N-Ligand Stabilized Oxomolybdenum Complexes

Organic ligands with donor functionalities such as nitrogen or oxygen atoms react readily with complexes of the type $MoX_2O_2(Solv)_2$ forming the octahedrally coordinated complexes. (Kühn, et al. 2000)

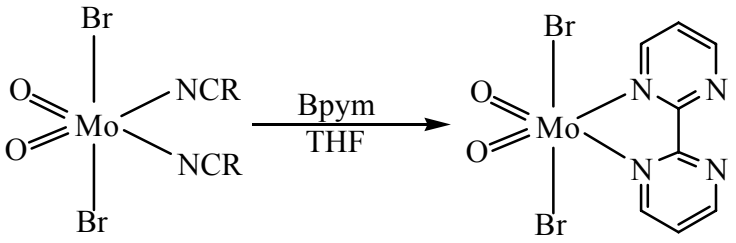

Figure.1.3.The The synthesis of N- ligand stabilized oxomolybdenum complexes (Source: Kühn, et al. 1999)

Reaction of solvent substituted $MoX_2O_2(Solv)_2$ complexes with bidentate nitrogen donor ligands leads to complexes of the type $MoX_2O_2L_2$ in nearly quantitative yields at room temperature within few minutes. $MoX_2O_2L_2$ systems with chelating nitrogen ligands display two important advantages: first, the two different ligand sets X and L can be easily varied in order to fine tune the ligand surrounding of the Mo (VI) center. Secondly, bidentate nitrogen donor ligands offer a great versatility in modifying the electron donor and acceptor properties of the ligands L. (Gonçalves, et al. 2001)

Mo=O IR vibrations of $MoX_2O_2L_2$ complexes were used to probe the influence of the ligands on the electronic properties of the metal and the Mo=O bond.

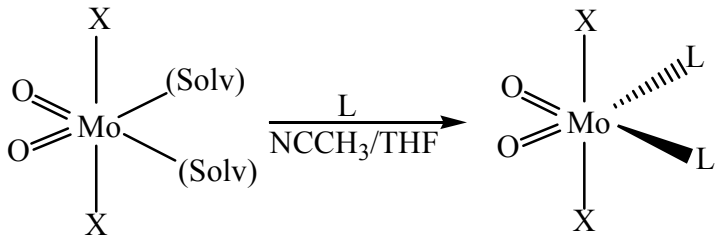

X= Cl, Br
(Solv)= $NCCH_3$, THF

L= Lewis base ligands

Figure 1.4. The reaction of solvent substituted complexes with Lewis base ligands
(Source: Kühn, et al. 2000)

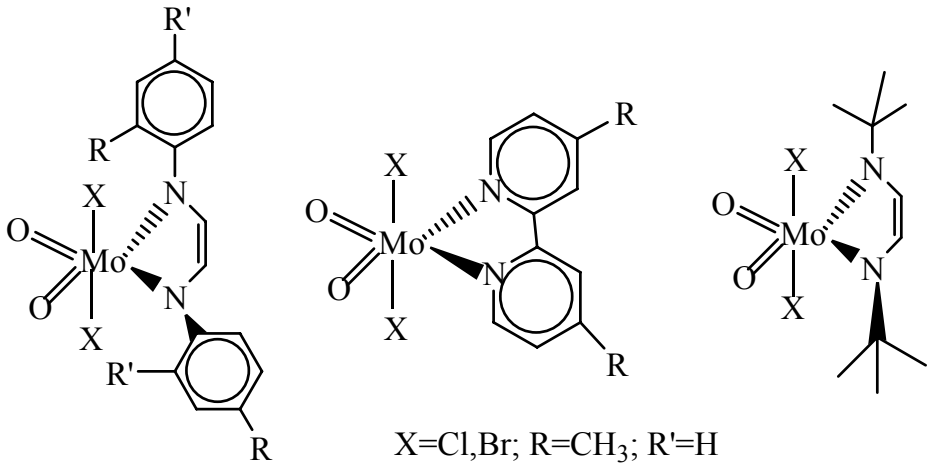

X=Cl,Br; R=CH_3; R'=H

Figure 1.5. Similar structures in the literature
(Source: Kühn, et al. 2000)

1.2.3 Olefin Epoxidation Catalyzed By Oxomolybdenum Complexes

1,2-Epoxycyclohexane, one of the most important organic intermediates, represents a rare combination of disparate qualities such as high reactivity and excellent selectivity. It is widely used in the synthesis of products such as enantioselective drugs, the pesticide propargite, epoxy paints, rubber promoters and dyestuff, and the market demand has been steadily increasing over recent years. Transition metal (Mo^{VI}, V^{V}, Ti^{IV}, Re^{VII}) containing catalysts for the epoxidation of cyclohexene have been widely investigated (Wang, et al. 2004). Mo(VI) is extremely important for epoxidation reactions, because the Lewis acidity of the catalysts has been pointed out as the key function of the catalyst. The major role of Mo(VI) ion is to withdraw electron from the peroxidic oxygens, making more susceptible to attack by nucleophiles such as olefins.

Though significant progress has been made in this field, major problems such as limited catalyst stability and rather difficult, and therefore expensive, synthetic procedures still remain to be solved. Designing a catalyst which gives rapid substrate conversion under mild conditions with high selectivity remains a challenge for these highly reactive systems. The process employs an easily prepared, inexpensive, and stable Mo-containing catalyst together with *tert*-butylhydroperoxide (TBHP).

step1

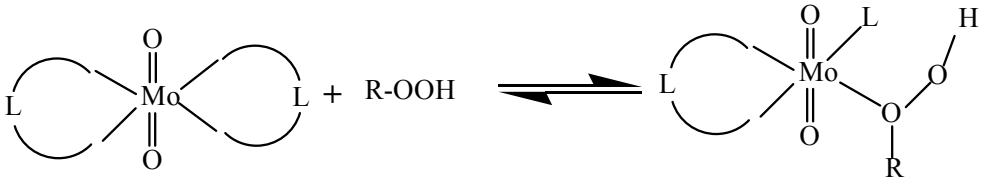

step2

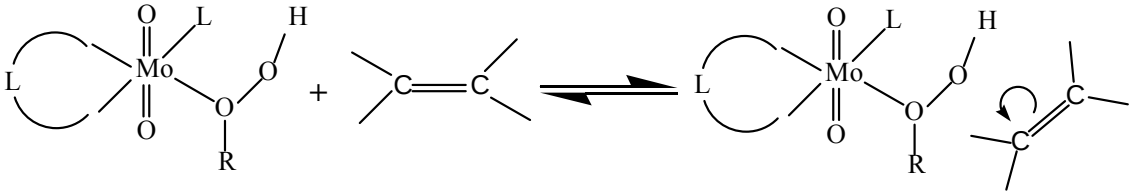

step3

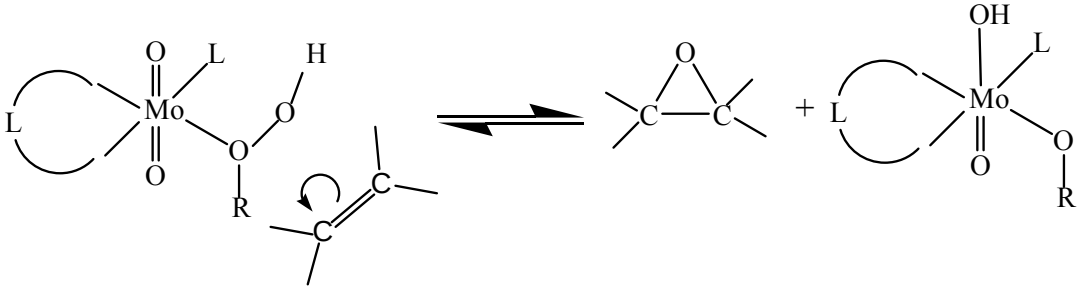

Figure 1.6. Suggested reaction pathway for cyclohexene epoxidation with TBHP catalyse by dioxomolybdenum complexes. (Source: Gnecco, et al. 2004)

(cont. on next page)

step4

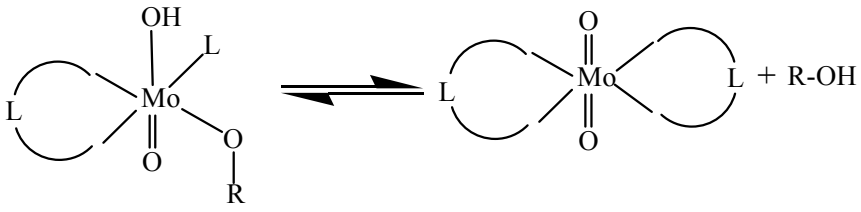

Figure 1.6. (cont.)

1.3. Enzymatic Applications of Oxomolybdenum Complexes

A variety of transition metals have found applications in biological systems by providing greater catalytic diversity which could not be achieved by the functional groups available in the sidechains of the aminoacids (Holm 1996). Organic forms of molybdenum are found in living matter, from bacteria to animals, including humans. Molybdenum is the only second row transition metal element required in biological reactions. Molybdenum is found in the active sites of so many enzymes due to the extreme solubility of molybdate salts. Molybdenum is the most abundant transition metal in seawater and the ratio of iron to molybdenum in the earth's crust is 3000:1 in favor of iron, but molybdenum is surprisingly 5-fold more abundant in sea water due to the greater solubility of molybdates in comparison to iron oxides. Therefore, it is not surprising that molybdenum has been incorporated widely into biological systems and these aspects of molybdenum chemistry accounts for why it is well suited to participate in the catalysis of certain types of biologically important reactions (Hille 2002, Sigel, et al. 2002, Hille 1996).

Enzymes containing molybdenum at their active sites are present in all forms of life, from ancient Achaeans to man. A number of well-known enzymes, including xanthine oxidase, nitrate reductase and sulfite oxidase, contain a mononuclear molybdenum center. Mononuclear molybdenum containing enzymes have the general function of catalyzing an oxygen atom transfer (OAT) to or from an acceptor/donor, with the metal oxidation state cycling between the +6 and +4 in the nitrogen, sulfur and carbon cycles and more than 40 enzymes were known. It is a necessary element, apparently for all species and only very small amounts are required. The vast majority of these enzymes

possess a Mo=O unit in their active sites are often referred to as oxomolybdenum enzymes (Hille 2002, Kisker, et al. 1997, Basu, et al. 2003, Enemark, et al. 2004).

1.3.1. Molybdenum cofactor (Moco)

Molybdenum itself is biologically inactive in biological systems unless it is complexed by a special cofactor. Apart from nitrogenases that contain an iron-molybdenum-sulfur cluster, the biological form of molybdenum present in almost all molybdenum-containing enzymes is an organic molecule known as the molybdenum cofactor (Moco), which contains a mononuclear molybdenum atom coordinated to an organic co-factor named molybdopterin (MPT) (Rajagopalan 1991). MPT contains a pterin, with pyrimidine and pyrazine rings. The pyrazine group is bonded to a pyran ring which carries both $-CH_2OPO_3^{2-}$ group and dithiolene group coordinated to molybdenum. Additional ligands that are found in the oxidazed Mo(VI) state of the cofactor includes one or two oxo ligands and/or a sulfido ligand and/or an amino acid residue such as serine or cysteine (Kisker, et al. 1997). The polar O, N, NH and NH_2 groups of MPT extensively take part in the formation of hydrogen bonds to complementary groups of the polypeptide chain. When phosphate is bonded to the nucleotide the extent of this hydrogen bonding is greatly increased. This hydrogen bond network would help for appropriate location of the catalytically active center within the polypeptide chain. The task of the cofactor is to position the catalytic metal molybdenum correctly within the active center, to be able to control its redox behaviour, and to take part in its pterin ring system in electron transfer to or from the Mo atom (Kisker, et al. 1997, Basu, et al. 2003 and Enemark, et al. 2004).

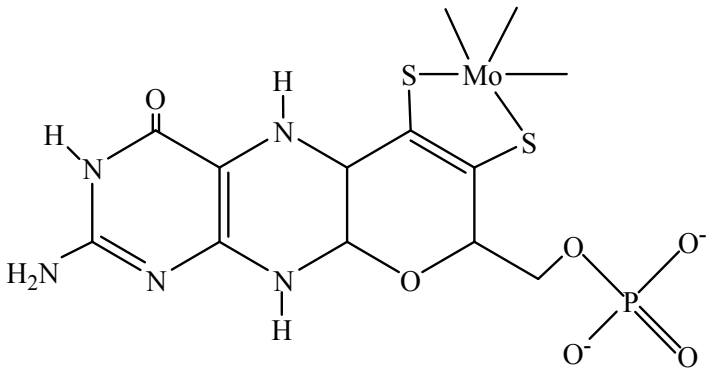

Figure 1.7. Structure of the molybdopterin

1.3.2. Mononuclear Molybdenum Enzymes

The majority of molybdenum enzymes can be classified (Hille 2002, Sigel, et al. 2002, Hille 1996) into three families each with a distinct active-site structure and type of reaction catalyzed: (1.1) molybdenum hydroxylases with a monooxo-molybdenum center belong to xanthine oxidase (XO) family, (1.2) molybdenum oxotransferases with a dioxomolybdenum center belong to the sulphite oxidase (SO) family (George, et al. 1989-1996, Hille 1996, Kisker, et al. 1997), and (iii) dimethyl sulfoxide (DMSO) reductase. Sulfite oxidase catalyzes the transformation of sulfite to sulfate, a reaction that is necessary for the metabolism of sulfur-containing amino acids, such as cysteine. Xanthine oxidase catalyzes the breakdown of nucleotides (precursors to DNA and RNA) to form uric acid, which contributes to the antioxidant capacity of the blood (McAlpine, et al. 1997, Bray, et al. 2000, Li, et al. 2000, George, et al. 1996-1999). Of these enzymes, only sulfite oxidase is known to be crucial for human health (Enemark, et al. 2004). Among 40 molybdoenzymes known, only four occur in humans and plants. These enzymes are; sulfite oxidase, nitrate reductase, xanthine oxidase, aldehyde oxidase. The crystal structures of sulphite oxidase (Kisker, et al. 1997), xanthine oxidase and nitrate reductase (Schultz, et al. 1993) have been determined. In humans, the molybdenum enzymes xanthine oxidase, sulfite oxidase and aldehyde oxidase are involved in the human diseases of gout, combined oxidase deficiency and radical damage following cardiac failure. All plants need molybdenum in nitrate reductase for proper nitrogen assimilation. In industrial catalysis, molybdenum is employed by the petroleum refining industry in multiple hydrotreating processes (Hille 2002).

Functionally, molybdoenzymes catalyse a net oxygen atom transfer reaction shown as below (1.1).

$$X + H_2O \rightleftharpoons XO + 2H^+ + 2e \qquad (1.1)$$

The oxygen atom, either derived from or incorporated into water, to or from a substrate in a two-electron reduction and this net reaction is considered to be a two-electron process. Common to all molybdenum enzymes, the metal centre functions as an electron-transferring unit regardless of the nature of the reaction catalyzed and there is a cycling between the oxidized Mo(VI) and the reduced Mo(IV) states of the enzyme. It is possible to consider the overall reaction mechanism as consisting of a coupled pair of reductive

and oxidative half-reactions, determined by the reduction of Mo(VI) and oxidation of Mo(IV), respectively. It is likely that the molybdenum undergoes a direct two-electron change in oxidation state during the half-reaction due to the two-electron redox reaction catalyzed by the enzyme followed by either addition or removal of electrons at the Mo, by means of electron transfer between the Mo and the second redox center (Hille 1996, Kisker, et al. 1997, Basu, et al. 2003, George, et al. 1989).

Xanthine oxidase (XO) family enzymes contain oxothioMo-center, O-Mo-S. They have been known as the enzymes that catalyze the hydroxylation of substrates in the presence of an electron acceptor (Hille 1996). Sulphite oxidase (SO) family including DMSO reductase and related enzymes contain dioxoMo-center, O-Mo-O, in contrast to the S-Mo-O unit in the XO family. These types of molybdoenzymes were known to function via an oxygen atom transfer process (Kisker, et al. 1997).

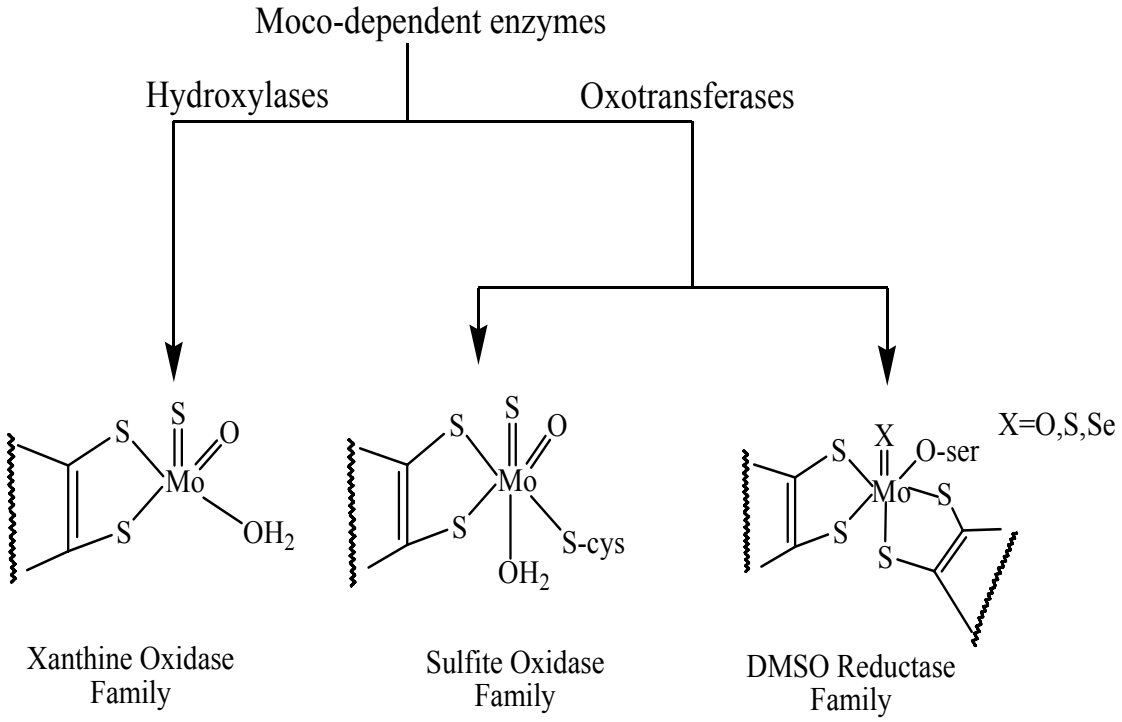

Figure 1.8. Hill classification-mononuclear molybdoenzymes
(Source: Hille 1996)

1.3.3. Oxomolybdenum Compounds as Molybdoenzymes

Mononuclear molybdenum containing enzymes catalyze a wide variety of reactions such as the reduction of nitrate to nitrite, reduction of dimethyl sulfoxide to dimethyl sulfide, reduction of arsenate to arsenite, or the oxidation of sulfite to sulfate (Hille 1996). These reactions play important roles in the global cycling of elements such as nitrogen, sulfur, arsenic and carbon. The vast majority of enzymes possess a Mo=O unit in their active sites are often referred to as oxomolybdenum enzymes. The presence of a Mo(VI)=O fuctional moiety is an essential future. The catalytic reactions take place at the molybdenum center, which is coordinated by the ene-dithiolate moiety of one or two pyranopterin cofactors.

The mechanisms of enzymes from the sulfite oxidase and the dimethyl sulfoxide (DMSO) reductase families are thought to involve direct oxygen atom transfer between the substrate and the molybdenum center (Sigel, et al. 2002, Hille 1996). In these reactions H^+, O^{2-} or HO^-, and electrons transfer between substrate molecules and molybdenum atoms and groups at the active centers. The chemistry involved is the acid-base and redox chemistry of molybdenum. The active site is a coordinately unsaturated molybdenum atom in a sulfur-ligand environment. Mo=O groups are found to be surprisingly labile, the metal centre is able to act as a catalyst for oxygen atom transfer to and from suitable acceptors and donors. Sulfite oxidases and nitrate reductases effect the substrate transformations through interconversion of $Mo^{VI}O[O]$ ([O]=active oxygen) and $Mo^{IV}O$ centers, while members of the DMSO reductase family exploit $Mo^{VI}[O]$ and Mo^{IV} centers in their catalytic centers. There are structural (Basu, et al. 2003, Kisker, et al. 1997, Li, et al. 2000, McAlpine, et al. 1998 and Ellis, et al. 2001), spectroscopic (Garton, et al. 2000, Astashkin, et al. 2000), kinetic (Schultz, et al. 1995) and theoretical (Thapper, et al. 2002) evidence for these reactions.

Several mononuclear oxomolybdenum(VI) and oxomolybdenum(IV) compounds have been synthesized (Enemark, et al. 2004, Schultz, et al. 1993, Das, et al. 1994, Chaudhury, et al. 1996, Ueyama, et al. 1996, Young, et al. 1996, Laughlin, et al. 1996, Lim, et al. 2001) to model the oxomolybdenum enzymes. These achievements by inorganic chemists provided a better understanding for the reactivity of the molybdenum cofactors and mechanisms of oxygen atom transfer reactions. The mechanism proposed for the oxygen atom transfer reaction involves a transition state where the molybdenum

atom and the substrate are bridged by the oxygen atom that is either entering or leaving the coordination sphere of the molybdenum atom (Lorber, et al. 1997, Tucci, et al. 1998). The catalytic activity of the enzyme is expected to be considerably influenced by the direct coordination environment of the molybdenum atom (Tong, et al. 1998, Tong, et al. 1999). The presence of a molybdenumpterin (dithiolene) ligand is present in all molybdenum enzymes. A number of $Mo^{VI}O_2$ complexes have been prepared as structural and functional models of molybdenum active sites (Enemark, et al. 2004, Holm 1987). Most of them were neutral compounds that contained weaker electron-donating ligand such as dimethyldithiocarbamate (S_2CNMe_2), 2,6-bis(2,2-diphenyl-2-marcaptoethanyl)pyridyne (dmp), and N,N'-dimethyl-N,N'-bis(2- mercaptophenyl)-ethylenedimin (Sphe). Due to the strong Lewis acidities and weak basicties of the oxo group, the molybdenum centers the $Mo^{VI}O_2$ units have short Mo^{VI}=O bond distances. Oxotransferase enzymes catalyze oxygen atom transfer to or from a biological oxygen acceptor or donor (1.2).

$$[Mo^{VI}O_n]^{2+} + X \rightleftharpoons [Mo^{IV}O_{n-1}]^{2+} + XO \quad (n=1,2) \qquad (1.2)$$

$Mo^{VI}O_2$ bis(thiolene) complexes such as $[MoO_2(mnt)_2]^{2-}$ (mnt=1,2-dicyano-1,2-ethylenedithiolate) $[MoO_2(bdt)_2]^{2-}$ (bdt = benzene-1,2-dithiolate) (George, et al. 1989) were reported as examples of oxotransferases including DMSO reductase family and sulfite oxidase (Hille 1996, Holm 1987). Isotope labeling experiments have revealed that the oxygen atom which is removed from the substrate coordinates to the molybdenum atom in the oxidized state of the enzyme in DMSO reductase. Therefore the presence of a Mo^{VI}=O functional moiety is essential for these group of enzymes (Schultz, et al. 1993, Das, et al. 1994, Chaudhury, et al. 1996, Young, et al. 1996, Laughlin, et al. 1996).

More recently, molybdoenzymes of the type, $[MoO_2(L^H)_2]^{2-}$, $[MoO_2(L^S)_2]^{2-}$, $[MoO_2(L^O)_2]^{2-}$, (L^H=cyclohexene-1,2-dithiolate, L^S=2,3-dihydro-2H-thiopyran-4,5-dithiolate, L^O= 2,3-dihydro-2H-pyran-4,5-dithiolate) in which the functional {Mo(VI)O_2}/ {Mo(IV)O} system stabilized by N,O- and N,S- donor ligands have been reported (Sugimoto, et al. 2005).

CHAPTER 2

EXPERIMENTAL STUDY

2.1. Experimental Techniques for Handling Air-Sensitive Compounds

All reactions carried out in this study are air and moisture sensitive therefore Vacuum-Line and Schlenk Technique is used for all experiments.

2.2. The Vacuum-Line Technique

2.2.1 The Double Manifold

If you wish to carry out reactions under dry and inert conditions, a double manifold is an extremely useful piece of apparatus (Figure 2.1.) (Leonard, et al. 1995).

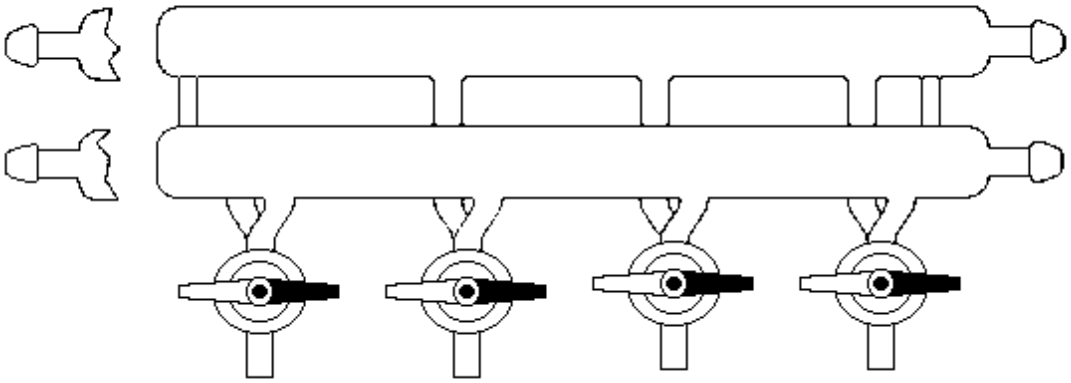

Figure 2.1. The double manifold.

The manifold consists of two glass barrel. One barrel of the manifold is connected to a high vacuum pump another to dry inert gas (Figure 2.2.). Thus, at the turn of the tap, equipment connected to the manifold can be alternately evacuated or filled with inert gas.

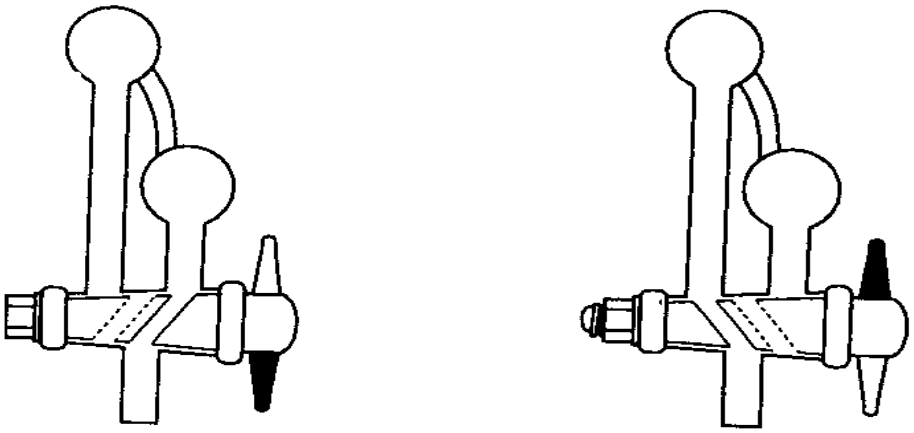

Tap switched to vacuum **Tap switched to inert gas**

Figure 2.2. Cross section through a double oblique tap.

2.2.2. The Schlenk Technique

To use a schlenk glassware provides facility during the reactions under N_2, with the schlenk tube one can transfer a solid or liquid in an atmosphere of an inert gas, such as nitrogen or argon (Shriver 1969, Barton, et al. 1963).

The basic and simplest schlenk tube is shown in Figure 2.3.The schlenk tube is stoppered and evacuated by pumping through D.By introducing the inert gas through A the tube is filled with the inert gas. The tap is turned through 90° to let gas pass through the tail part and then is turned through 90° to allow gas into the flask.

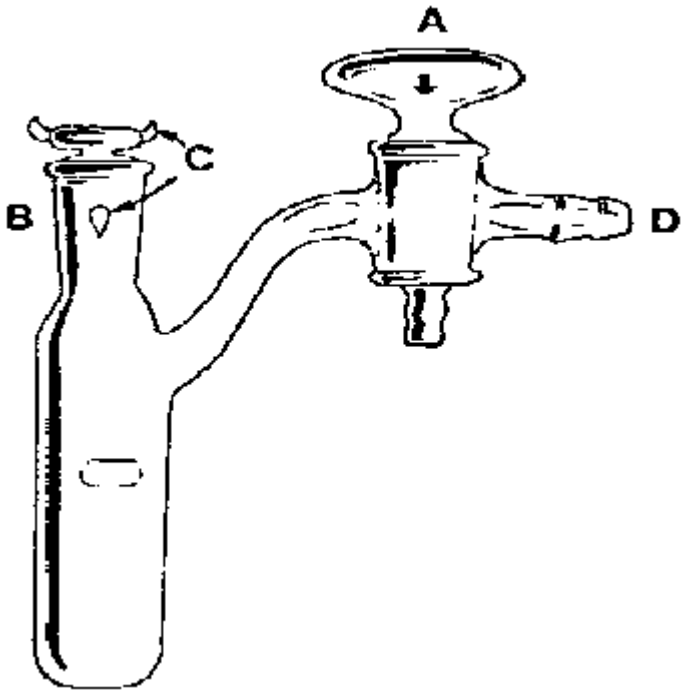

Figure 2.3. The schlenk tube.

2.3. Purification of Solvents

The solvents used are purified, dried under nitrogen by distillation system. A solvent still is used for this purpose (Shriver 1969, Barton, et al. 1963, Harwood and Moody 1989). This system provides removing the small amount of impurities and any water from the solvent. An example of a solvent still is shown in Figure 2.4.

It consist of a large distillation flask, connected to a reflux condenser via a piece of glassware which can simply be a pressure equalizing funnel modified by the inclusion of a second stopcock. Since the production of very dry solvents usually requires the exclusion of air from the apparatus, the still is fitted so that it can be operated under an inert atmosphere. Firstly, drying agent and solvent are added to the distillation flask under N_2. With the stopcock A open, the solvent simply refluxes over the drying agent. When the stopcock A is closed, the solvent vapour passes up the narrow tube and dry solvent collects in the central piece of the apparatus. When the required volume of the solvent has been collected, it can be run off through the stopcock B. The solvents were prepared for the use as described below.

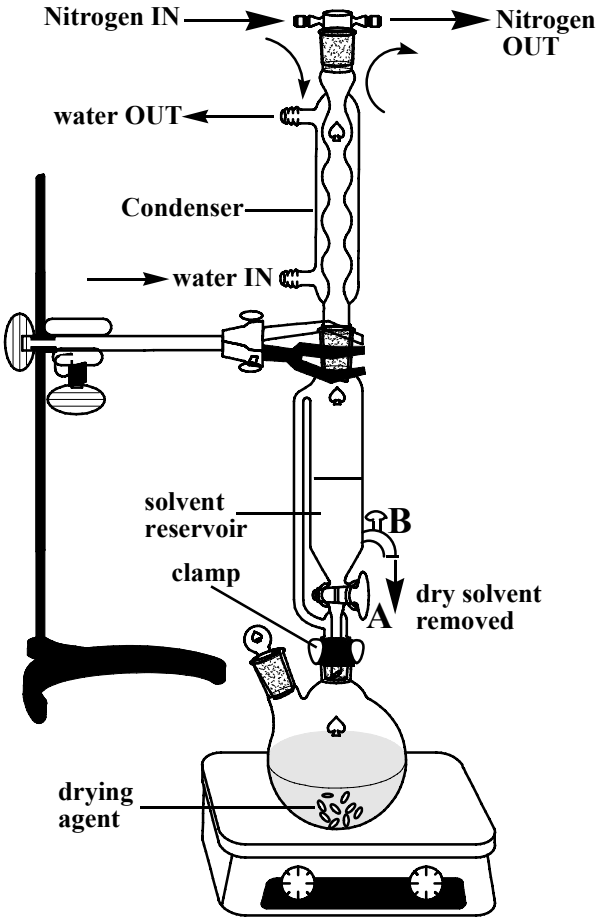

Figure 2.4. Solvent still.

Tetrahydrofuran: The sodium wire and benzophenone are added to the solvent and it is refluxed under inert atmosphere until the deep blue color persists and then the solvent is distilled and stored onto 4A molecular sieves.

Dichloromethane: The solvent is refluxed over calcium hydride and distilled and then stored onto 4A molecular sieves.

Hexane: The same procedure is performed in purification of dichloromethane.

2.4. Materials and Methods

All reactions, synthetic operations, and manipulations were carried out under an oxygen-free and water-free nitrogen atmosphere using standard schlenk techniques, a high-vacuum/gas double line manifold. Reactions were monitored by thin layer chromatography (TLC). Solvents were dried by standard procedures, distilled and kept under nitrogen over 4A molecular sieves. All glassware was oven dried at 120 ºC and

schlenk ware was further purged by repeated evacuation and inert gas flushes prior to use. The new compounds were usually purified by CH_2Cl_2 / n-Hexane.

Reagents: Dichloro, Methyl, nitro group functionalized diamines and 1,2-phenylenediamine were obtained from Fluka. N-phenyl and tetra-methyl group substituted diamines were obtained from Aldrich. 1,4-phenylenediamine was obteined from Acros. Tetrahydrofuran were obtained from Merck. Dichloromethane was obtained from Riedel. Hexane was obtained from Carlo Erba. The starting material $[MoO_2Cl_2]$ was purchased from Aldrich. $[MoO_2Cl_2(THF)_2]$ was prepared according to the literature method (Kuhn, et al. 2001, Herdtweck, et al. 2002). All yields are based on the starting material containing compound.

Instruments: The products were characterized by IR, ^{1}H-NMR spectroscopy and Elemental analysis. Infrared spectra were recorded on as KBr pellet on a Perkin-Elmer model (100) FT-IR spectrometer after grinding the sample with KBr. ^{1}H-NMR spectra were recorded in DMSO on Varian AS 400 Mercury Plus at Ege University. Elemental analyses were performed on Leco CHNS 932.

Computational Methods: The geometry optimizations of all complexes were performed at molecular mechanics, PM3 and B3LYP/LACVP levels of theory. The optimized geometries obtained in the previous step were characterized by utilizing vibrational frequency analyses at PM3 and B3LYP/LACVP levels. All calculations throughout the study have been carried out with SPARTAN08 at Ege University.

2.5. Syntheses

2.5.1. Reaction of $[MoO_2Cl_2]$ with $[(H_2N)_2C_6H_4]$ (1)

1,2-phenylenediamine 0.27 g (2.50mmol) was added to a solution of 0.50 g (2.51 mmol) $[MoO_2Cl_2]$ in 20 ml dry THF. The colour of the solution changed to dark red. Reaction was monitored by thin layer chromatography (TLC). After stirring the mixture for further 30 min. at room temperature the reaction product precipitated as solid. The solvent was evaporated to dryness. The obtained solid was washed with CH_2Cl_2 and crystallization with n-hexane. Finally, the product was dried under vacuum. Compound (I) was obtained as purple solid in 83% yield.

2.5.2. Reaction of $[MoO_2Cl_2]$ with $[(H_2N)(HNC_6H_5)C_6H_4]$ (2)

N-phenyl-1,2-phenylenediamine 0.44 g (2.38 mmol) was added to a solution of 0.48 g (2.41 mmol) $[MoO_2Cl_2]$ in 20 ml dry THF. The colour of the solution changed to dark red. Reaction was monitored by thin layer chromatography (TLC). After stirring the mixture for further 30 min. at room temperature the reaction product precipitated as solid. The solvent was evaporated to dryness. The obtained solid was washed with CH_2Cl_2 and crystallization with n-hexane. Finally, the product was dried under vacuum. Compound (II) was obtained as black solid in %81 yield.

2.5.3. Reaction of $[MoO_2Cl_2]$ with $[(H_2N)_2C_6H_5(CH_3)]$ (3)

4-Methyl-1,2-phenylenediamine 0.30 g (2.46 mmol) was added to a solution of 0.49 g (2.46 mmol) $[MoO_2Cl_2]$ in 20 ml dry THF. The colour of the solution changed to dark red. Reaction was monitored by thin layer chromatography (TLC). After stirring the mixture for further 30 min. at room temperature the reaction product precipitated as solid. The solvent was evaporated to dryness. The obtained solid was washed with CH_2Cl_2 and crystallization with n-hexane. Finally, the product was dried under vacuum. Compound (III) was obtained as black solid in 86% yield.

2.5.4. Reaction of $[MoO_2Cl_2]$ with $[(H_2N)_2C_6H_3(NO_2)]$ (4)

4-Nitro-1,2-phenylenediamine 0.34 g (2.22 mmol) was added to a solution of 0.44 g (2.21 mmol) $[MoO_2Cl_2]$ in 20 ml dry THF. The colour of the solution changed to dark brown. Reaction was monitored by thin layer chromatography (TLC). After stirring the mixture for further 30 min. at room temperature the reaction product precipitated as solid. The solvent was evaporated to dryness. The obtained solid was washed with CH_2Cl_2 and crystallization with n-hexane. Finally, the product was dried under vacuum. Compound (IV) was obtained as dark grey solid in 80% yield.

2.5.5 Reaction of $[MoO_2Cl_2]$ with $[(H_2N)_2C_6H_4]$ (5)

1,4-phenylenediamine 0.22g (2.03mmol) was added to a solution of 0.40 g (2.01 mmol) $[MoO_2Cl_2]$ in 20 ml dry THF. The colour of the solution changed to black. Reaction was monitored by thin layer chromatography (TLC). After stirring the mixture for further 30 min. at room temperature the reaction product precipitated as solid. The solvent was evaporated to dryness. The obtained solid was washed with CH_2Cl_2 and crystallization with n-hexane. Finally, the product was dried under vacuum. Compound (V) was obtained as black solid in 89% yield.

2.5.6. Reaction of $[MoO_2Cl_2]$ with $[(H_2N)(HNC_6H_5)C_6H_4]$ (6)

N-phenyl-1,4-phenylenediamine 0.44 g (2.39 mmol) was added to a solution of 0.48 g (2.41 mmol) $[MoO_2Cl_2]$ in 20 ml dry THF. The colour of the solution changed to dark green. Reaction was monitored by thin layer chromatography (TLC). After stirring the mixture for further 30 min. at room temperature the reaction product precipitated as solid. The solvent was evaporated to dryness. The obtained solid was washed with CH_2Cl_2 and crystallization with n-hexane. Finally, the product was dried under vacuum. Compound (VI) was obtained as green solid in 84% yield.

2.5.7. Reaction of $[MoO_2Cl_2]$ with $[(H_2N)_2C_6H_2Cl_2]$ (7)

2,6-dichloro-1,4-phenylenediamine 0.49 g (2.77 mmol) was added to a solution of 0.55 g (2.76 mmol) $[MoO_2Cl_2]$ in 20 ml dry THF. The colour of the solution changed to black. Reaction was monitored by thin layer chromatography (TLC). After stirring the mixture for further 30 min. at room temperature the reaction product precipitated as solid. The solvent was evaporated to dryness. The obtained solid was washed with CH_2Cl_2 and crystallization with n-hexane. Finally, the product was dried under vacuum. Compound (VII) was obtained as green solid in 88% yield.

2.5.8. Reaction of $[MoO_2Cl_2]$ with $[(H_2N)_2C_6(CH_3)_4]$ (8)

2,3,5,6-tetramethyl-1,4-phenylenediamine 0.37 g (2.22 mmol) was added to a solution of 0.44 g (2.21 mmol) $[MoO_2Cl_2]$ in 20 ml dry THF. The colour of the solution changed to dark green. Reaction was monitored by thin layer chromatography (TLC). After stirring the mixture for further 30 min. at room temperature the reaction product precipitated as solid. The solvent was evaporated to dryness. The obtained solid was washed with CH_2Cl_2 and crystallization with n-hexane. Finally, the product was dried under vacuum. Compound (VIII) was obtained as green solid in 83% yield.

CHAPTER 3

RESULT AND DISCUSSION

3.1. Synthetic Studies

The solvent-stabilized compound $[MoO_2Cl_2(THF)_2]$ was obtained according to the literature method (Kuhn, et al. 2001, Herdtweck, et al. 1999).

Reaction of $[MoO_2Cl_2]$ with o-phenylenediamine *o*-$(H_2N)_2C_6H_4$ (1) and substituted o-phenylenediamines; [*o*-$(H_2N)(HNR)C_6H_4$] (2) , [*o*-$(H_2N)_2C_6H_5R$] (3-4) (R= C_6H_5, CH_3, NO_2 respectively) in THF produced N,N'-bis-(chloro)dioxomolybdenum(VI) compounds, $[MoO_2Cl_2(o\text{-}(HN)_2C_6H_4)]$, $[MoO_2Cl_2(o\text{-}(HN)(NC_6H_5)C_6H_4)]$, $[MoO_2Cl_2(o\text{-}(HN)_2C_6H_4(CH_3))]$, and $[MoO_2Cl_2(o\text{-}N_2C_6H_4(NO_2))]$ as the major products. This is such an expected result as the previously reported related reactions between $[MoO_2Cl_2]$ with bidentate nitrogen donor ligands resulted in the formation of N,N'-bis-(chloro)dioxomolybdenum(VI) compounds, in nearly quantitative yields. These compounds were the examples of dioxomolybdenum (VI) compounds containing bidentate aryl-nitrogen donor ligands. They could easily be separated from the reaction mixture and purified (e.g., from excess of ligand) by washing with dichloromethane and hexane. The product complexes are in general significantly less soluble than the starting materials. The resulting complexes are stable and can be handled in air.

Reaction of $[MoO_2Cl_2]$ with p-phenylenediamine *p*-$(H_2N)_2C_6H_4$ (5) and substituted p-phenylenediamines; [*p*-$(H_2N)(HNR)C_6H_4$] (6) , [*p*-$(H_2N)_2C_6H_4R_2$] (7) [*p*-$(H_2N)_2C_6R_4$] (8) (R= C_6H_5, Cl, CH_3, respectively) in THF produced N-bis-(chloro)dioxomolybdenum(VI) compounds, $[MoO_2Cl_2(p\text{-}(NH)_2C_6H_4)]$, $[MoO_2Cl_2(p\text{-}(HN)(HNC_6H_5)C_6H_4)]$, $[MoO_2Cl_2(p\text{-}H_2NNC_6H_4Cl_2)]$, $[MoO_2Cl_2(p\text{-}H_2N(HN)C_6(CH_3)_4)]$ as the major products. The reaction of p-phenylenediamine and derivatives with $[MoO_2Cl_2]$ produced dioxo-monodentate Mo(VI) compounds. Although the resulting complexes were dioxomolybdenum (VI) compounds containing bidentate aryl-nitrogen donor ligands surprisingly, they showed coordinate via one nitrogen atom. They could easily be separated from the reaction mixture and purified (e.g., from excess of ligand) by

washing with dichloromethane and hexane. The product complexes are in general significantly less soluble than the starting materials. The resulting complexes are stable and can be handled in air.

3.2. Spectroscopic Studies

The IR spectra data for the complexes **(I)-(VIII)** are given in Table 3.1. And their spectra are shown in Figures B.1. - B.8. Five compounds (**I**, **II**, **III**, **V**, **VI** and **VIII**) exhibited the expected absorptions due to the Mo-N bond (550-450 cm^{-1} due to $\nu_{(MoN)}$) (Zekri, et al. 2000, Tuczek, et al. 2003). The compounds for **IV** and **VII** revealed the expected peak for Mo=N bond. A value of 1200-1300 cm^{-1} for Mo=N has been suggested (Dehnicke and Strahle 1981).

The IR sectra of **(I)-(VIII)** show a pair of two strong bands at about 900 and 979 cm^{-1} arising from symmetric and asymmetric [MoO_2] stretching vibrations, respectively (Kühn, et al. 1993). The infrared spectra of the new complexes exhibited, beside typical ligand vibrations, these two strong absorptions which are attributed to the symmetric and asymmetric Mo=O vibrations of the C_{2v} cis-MoO_2^{2+} groups, thus there is confirming the formation of mononuclear molybdenum (VI) complexes.

The presence of phenylenediamine is indicated by a strong or medium ν(NH). The two vibrations at 3500-3200 cm^{-1} from ν_s(NH) and ν_{as}(NH) of the NH_2 groups of the free ligands have disappeared in the IR spectra of *o*-phenylenediamine complexes. NH_2 groups which are attached to molybdenum (VI) center observed as secondary amines. Their IR spectra showed the loss of one proton of the amine for three *o*-phenylenediamine complexes. 4-Nitro-*o*-phenylenediamine derivative exhibited the expected peak for the suggested M=N bond.

In three *p*-phenylendiamine complexes, it is observed the expected N-H and NH_2 peaks. 2,6-dichloro *p*-phenylenediamine derivative revealed the expected peak for Mo=N bond.

Table 3.1. Some important IR data for the complexes (cm^{-1})

Complex	N-H	ν_s- ν_{as} N-H (NH_2)	Mo=O	Mo=N	Mo-N
(I)	3444		958-899		517
(II)	3311		979-927		483
(III)	3427-3300		954-908		493
(IV)			968-938	1203	
(V)	3419	3500-3300	951-910		494
(VI)	3400-3315		976-910		498
(VII)		3423 -3368	953-905	1318	
(VIII)	3346	3200-3300	951-903		458

The ^{1}H-NMR spectra data for the complexes are given in table 3.2 and their spectra are shown in figures A.1-A.8.

Generally NH_2 and NH protons appear in the range δ 11.14-13.15 p.p.m. (McCleverty, et al. 1983) for o-phenylenediamines dioxomolybdenum(VI) compounds, this N-H peak is observed. All of the ^{1}H-NMR spectra for the products obtained from the reactions of $[MoO_2Cl_2]$ with ; [*o*-$(H_2N)_2C_6H_4$] **(I)**, and substituted o-phenylenediamines; [*o*-$(H_2N)(HNC_6H_5)C_6H_4$] **(II)**, [*o*-$(H_2N)_2C_6H_5CH_3$] **(III)** displayed N-H peaks. Only $[MoO_2Cl_2$(*o*-$N_2C_6H_5NO_2)]$ o-phenylenediamine derivative did not show neither NH nor NH_2 protons. Therefore, a Mo=N type binding could be suggested for this complex **(IV)**. This could be explained by the electron withdrawing effect of the NO_2 group. There are broad signals typical of amine protons were observed in the ^{1}H-NMR spectra of the new p-phenylenediamines dioxomolybdenum(VI) compounds. The ^{1}H-NMR spectra obtained the signals attributable to amine appear as singlets in the regions δ 3-2 ppm, assigned to the amine NH protons. The ^{1}H-NMR results included that the $[MoO_2Cl_2$(*p*-$H_2NHNC_6H_4)]$ **(V),** $[MoO_2Cl_2$(*p*-$(HN)(HNC_6H_5)C_6H_4)]$ **(VI)** and $[MoO_2Cl_2$(*p*-$H_2N(HN)C_6(CH_3)_4)]$ **(VIII)** complexes displayed both NH_2 and NH protons unlike, $[MoO_2Cl_2$(*p*-$H_2NNC_6H_4Cl_2)]$ **(VII)** derivative only showed NH_2 protons. Therefore, Mo=N type of binding could be suggested for this complex **(VII)** This could be explained by the electron withdrawing effect of two electron withdrawing Cl substituents at 2,6 position in the *p*-phenylene ring.

Table 3.2. ^{1}H-NMR data for the complexes

Complex	□[b]/ p.p.m	A[c]	Assignment
	8.11	2	s, $\underline{H}NC_6H_4$
I	6.98-6.77	4	m,$NC_6\underline{H}_4$
	14.04	1	s, $\underline{H}NC_6H_4$
II	8.16-6.10	8	m,$HNC_6\underline{H}_4NC_6\underline{H}_4$
	6.99-6.55	3	m, $NC_6\underline{H}_3CH_3$
	9.34,8.47	1,1	s,s, $\underline{H}N\underline{H}NC_6H_3CH_3$
III	2.49	3	s, $NC_6H_3C\underline{H}_3$
	7.92-7.79	2	$NC_6\underline{H}_3NNO_2$
IV	6.79	1	s,$NC_6\underline{H}_3NNO_2$
	8.49	1	s, $H_2N\underline{H}NC_6H_4$
	7.03	4	s, $H_2NHNC_6\underline{H}_4$
V	3.54	2	s, $\underline{H}_2NHNC_6H_4$
	9.64	1	s, $\underline{H}NC_6H_4HNC_6H_5$
	8.25	1	s, $HNC_6H_4\underline{H}NC_6H_5$
VI	7.23-6.80	8	m,$HNC_6\underline{H}_4NHC_6\underline{H}_5$
	6.94	2	s, $H_2NC_6\underline{H}_2Cl_2N$
VII	3.32	2	s, $\underline{H}_2NC_6H_4Cl_2N$
	7.41	1	m,$H_2NC_6(CH_3)_4N\underline{H}$
	3.41	2	m,$\underline{H}_2NC_6(CH_3)_4NH$
VIII	2.13	12	m,$H_2NC_6(C\underline{H}_3)_4NH$

^{13}C-NMR spectra of the novel complexes showed changes between the chemical shifts of the free and bonded ligands. This behavior can be explained by electron deficient of Mo center in the starting compound and coordination of N donor ligands. It demonstrated that phenylenediamine ligands influence the electron density at the metal center of these complexes. Carbons attached via N-Mo in the complexes displayed the shifted signals consistent with an increased electron density at the metal center.

Table 3.3. ^{13}C-NMR data for the complexes

COMPLEX	Shifts δ^b/ p.p.m.
I	162.81, 127.00, 119.50
II	148.47, 144.49, 143.40, 130.10, 129.05, 126.80, 120.82, 120.13, 117.01, 116.80
III	124.72, 122.57, 119.49, 115.88, 67.49, 63.55, 25.59
IV	147.15, 136.66, 123.17, 122.05, 116.68, 114.33
V	119.50, 67.75
VI	144.12, 143.49, 129.87, 124.87, 123.44, 120.97, 117.95, 117.41
VII	138.93, 126.28, 121.06, 118.69
VIII	140.46, 123.46, 14.96

Table 3.4. Elemental Analysis data for the complexes

Complexes	Emprical Formula (molecular weight) g/mole Calculated	%C	%H	%N
		Found (calculated)		
I	$C_6H_6N_2O_2Cl_2Mo$ (305.09)	22.74 (23.62)	3.59 (1.97)	8.41 (9.19)
II	$C_{12}H_9N_2O_2Cl_2Mo$ (381.19)	37.52 (37.80)	3.33 (2.62)	7.12 (7.36)
II	$C_7H_8N_2O_2Cl_2Mo$ (524.05)	25.12 (16.04)	4.15 (1.53)	7.65 (5.35)
IV	$C_6H_3N_3O_2Cl_2Mo$ (348.09)	21.62 (20.70)	3.04 (1.44)	12.40 (12.09)
V	$C_6H_7N_2O_2Cl_2Mo$ (306.09)	24.65 (23.54)	3.82 (2.29)	8.03 (9.17)
VI	$C_{12}H_{11}N_2O_2Cl_2Mo$ (382.19)	38.53 (37.71)	4.01 (2.88)	7.29 (7.34)
VII	$C_6H_4N_2O_2Cl_4Mo$ (373.98)	22.38 (19.27)	2.53 (1.1)	7.49 (7.5)
VIII	$C_{10}H_{15}N_2O_2Cl_2Mo$ (362.20)	31.27 (33.15)	4.95 (4.14)	6.67 (7.75)

3.3. Theoretical Studies

In this study, molecular mechanics (MM), semi empirical PM3 method and B3LYP, the most widely used hybrid functional of Density Functional Theory (DFT) methods, were employed. In MM, Newtonian mechanics is utilized for modeling molecular systems. The potential energy of all systems is calculated using force fields referring to the functional form and parameter sets, derived from both experimental data and high-level quantum mechanical calculations, exploited to describe the potential energy of a system of particles. As a brief, MM provide a fairly accurate "guess" at molecular geometry in terms of bond lengths, bond angles and torsion angles, provided that the molecule has already been represented in terms of a particular valence structure. Semi-empirical PM3 calculations provide a solid description of the geometries of transition-metal coordination compounds. PM3 can be recommended (with due caution) for preliminary structure determinations of transition-metal coordination compounds. Density functional theory (DFT) is a quantum mechanical theory in which the properties of a many-electron system can be determined by using functionals that spatially depends on electron density of the system. B3LYP hybrid functional is routinely applicable to determination of equilibrium and transition-state geometries and of vibrational frequencies (Hehre 2003).

It was shown in some earlier theoretical studies of molybdenum complexes that DFT method is suitable for geometry optimization and energy calculations of systems with multiple M–L bonds (Zaric, et al. 1997, Webster, et al. 2001, Z'miric´, et al. 2002, Kail, et al. 2006). Basis sets for the calculations of molybdenum complexes are given in the literature. Spin-restricted density functional theory (DFT) calculations were carried out for the molybdenum complexes using the DFT method with the hybrid exchange-correlation functional B3LYP (Becke 1993). Of the many available functionals, we have chosen B3LYP because it has provided accurate results for organic molecules in general and for Group 6 metal complexes containing N-donor ligands (Vlc'ek 2002). In the light of this view, B3LYP method was chosen to employ estimating structural parameters and vibrational frequencies for MoN, MoO and NH to provide support for experimentally obtained vibrational assignments.

After characterization of the complexes dioxomolybdenum phenylenediamines bearing bidentate nitrogen donors with synthetic and spectroscopic studies, it is expected that the coordination is either bidentate or monodentate. In order to determine the structure of coordination, the geometries of complexes were optimized using MM, PM3 and B3LYP methods. All geometry optimizations were carried out in vacuum utilizing the SPARTAN 08 computational chemistry suite. In DFT calculations, the LACVP and LACVP** basis sets, which is available in SPARTAN 08, were employed. These basis sets are combinations of other two basis sets. In both LACVP and LACVP**, molybdenum metal is described with the LANL2DZ basis set (Hay and Wadt 1985) and the remaining atoms are described with 6-31G and 6-31G(d,p) basis sets (McLean and Chandler 1980, Krishnan, et al. 1980) respectively. The PM3 optimized complex geometries were initially optimized at B3LYP/LACVP level of theory. Then, the geometries optimized at that level were re-optimized with B3LYP employing LACVP** basis set including polarization functions to obtain more improved complex geometries. In the optimized phenylenediamine molecules, consistency between DFT frequencies and experimental values were satisfactory.

MM optimized geometries of p-phenylenediamine and derivatives (**V-VIII**) deform the benzene ring as seen in Fig. 3.1. This must be an impossible conformation for a stable complex. Obviously, MM fails badly for such complexes. The instability of these types of geometries was proven by the B3LYP method as it pushed the Mo center from the benzene ring so that benzene can be planar. Hence, the bidentate coordination is not possible for p-phenylenediamine complexes (**V-VIII**) since this coordination needs to distort the benzene ring.

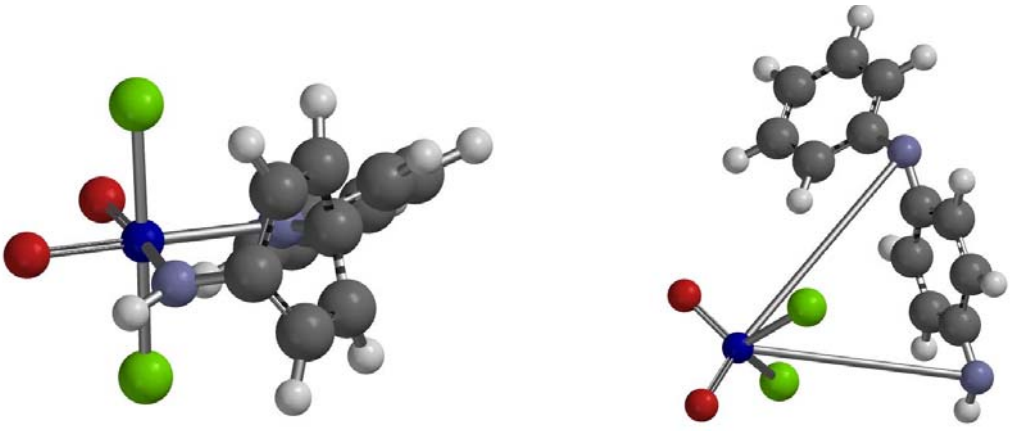

Figure 3.1.The optimized geometries with MM and DFT calculation for the complex **(VI),** respectively.

Unlike p-phenylenediamine complexes, the MM and DFT calculations pointed out that the bidentate structures are the most stable form of o-phenylenediamine complexes **(I-IV)** in the gas phase. N,N'-bis-(chloro)dioxomolybdenum(VI) compounds were observed.

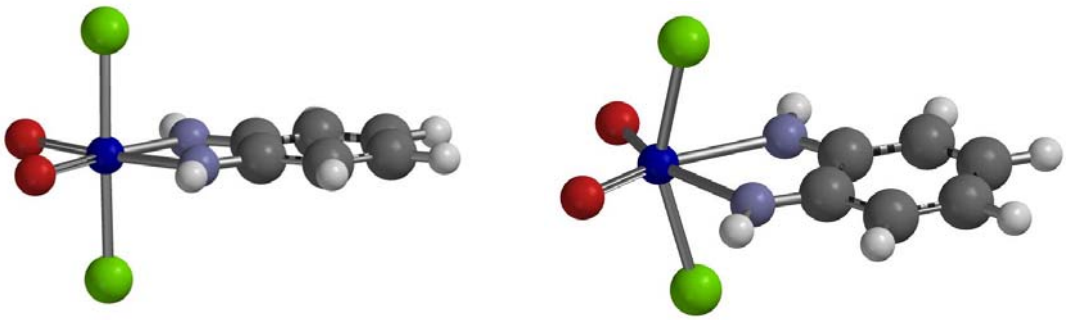

Figure 3.2.The optimized geometries with MM and DFT calculation for the complex **(I),** respectively

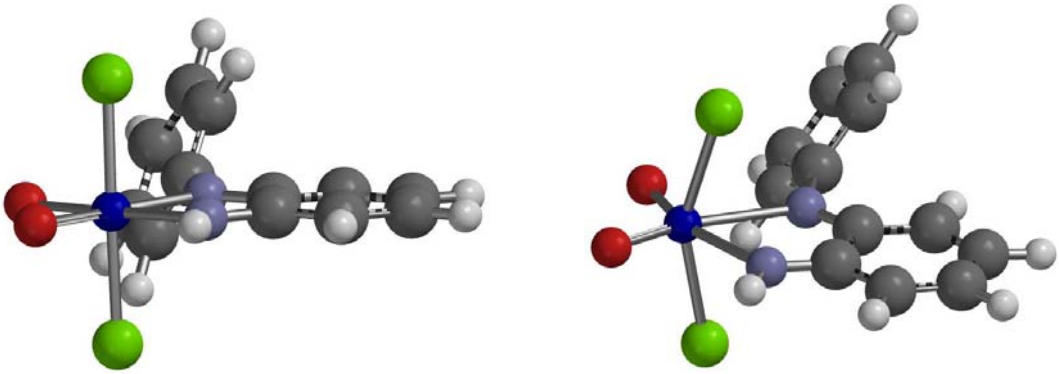

Figure 3.3.The optimized geometries with MM and DFT calculation for the complex **(II),** respectively

The vibrational frequencies of the optimized geometries for the complexes **(I-VIII)** were calculated at the B3LYP/LACVP** level. Initial geometries of all structures suggested by the experimental findings were fully optimized to their equilibrium geometries. Harmonic vibrational frequency calculations result in no imaginary frequencies, indicating that all structures are minima in the potential energy surface. The calculated frequencies (see below) for the complexes are given in Table 3.5. Although the numbers do not agree completely, the trends fit the experimental values. The characteristic symmetric and antisymmetric Mo=O stretchings of the complexes are

calculated about 971 and 1021 cm^{-1} in good agreement with the experimental values (980, 908 cm^{-1}) . The quality of the basis set, the theoretical method used, and the fact that a gaseous molecule is analyzed for the calculations may be responsible for the partial agreement.

Table 3.5. Some important IR DFT (B3LYP/LACVP**) calculated data for the complexes **(I-VIII)** (cm^{-1})

Complex	**N-H**	**ν_s- ν_{as} N-H (NH_2)**	**Mo=O**	**Mo=N**	**Mo-N**
I	3524		971-956		482
II	3533		971-962		486
III	3528-3531		976-995		519
IV			992-1021	1304	
V	3534	3618-3744	979-1004		495
VI	3537-3605		982-1004		564
VII		3556-3685	970-985	1307	
VIII	3544	3649-3771	978-1003		503

Thermodynamic calculations were performed in the gas phase at 298 K for the optimized complex geometries. Calculated enthalpies showed that all of the reactions are highly endothermic (see below). Experimentally, it was observed that there was a temperature drop during the course of all reactions, indicating the reactions are endothermic. This decrease in the temperature confirms that the experimental findings are in accordance with the theoretical calculations.

Table 3.6. ΔH calculations with DFT (B3LYP/LACVP**) for the complexes respectively, **(I-VIII)**

REACTION	**ΔH_r (kcal/mol)**
$MoO_2Cl_2 + o\text{-}(H_2N)_2C_6H_4 \longrightarrow [MoO_2Cl_2(HN)_2C_6H_4]$	753.17
$MoO_2Cl_2 + o\text{-}(H_2N)(HNC_6H_5)C_6H_4 \longrightarrow [MoO_2Cl_2(HN)(HNC_6H_5)C_6H_4]$	754.38
$MoO_2Cl_2 + o\text{-}(H_2N)_2C_6H_4CH_3 \longrightarrow [MoO_2Cl_2(HN)_2C_6H_4CH_3]$	753.66
$MoO_2Cl_2 + o\text{-}(H_2N)_2C_6H_4NO_2 \longrightarrow [MoO_2Cl_2(N)_2C_6H_4NO_2]$	1608.66
$MoO_2Cl_2 + p\text{-}(H_2N)_2C_6H_4 \longrightarrow [MoO_2Cl_2(H_2N)(HN)C_6H_4]$	374.71
$MoO_2Cl_2 + p\text{-}(H_2N)(HNC_6H_5)C_6H_4 \longrightarrow [MoO_2Cl_2(HN)(HNC_6H_5)C_6H_4]$	375.82
$MoO_2Cl_2 + p\text{-}(H_2N)_2C_6H_4Cl_2 \longrightarrow [MoO_2Cl_2(H_2N)NC_6H_4Cl_2]$	797.25
$MoO_2Cl_2 + p\text{-}(H_2N)_2C_6H_4(CH_3)_4 \longrightarrow [MoO_2Cl_2(H_2N)(HN)C_6H_4(CH_3)_4]$	374.18

In the DFT B3LYP calculations, LACVP and LACVP** basis sets were employed. The latter includes polarization functions on hydrogen and other heavy atoms except for metal atom. Introduction of polarization functions with LACVP** basis set led to energetically more favorable optimized complex geometries. Tables 3.7 and 3.8 show some selected bond distances and bond angles, respectively. There were significant changes in bond distances and bond angles of the complex molecules.

Table 3.7. Polarization effect on atom distances with comparing basis sets (LACVP /LACVP**) for the complexes respectively, **(I-VIII)**

COMPLEX	**DISTANCES(Å)**					
	Mo-O		Mo-Cl		Mo-N	
	LACVP	**LACVP****	**LACVP**	**LACVP****	**LACVP**	**LACVP****
I	1.74	1.71	2.46	2.41	2.33	2.40
II	1.73	1.71	2.45	2.41	2.45	2.33
III	1.74	1.71	2.46	2.41	2.32	2.40
IV	1.72	1.7	2.43	2.37	2.42	2.52
V	1.73	1.71	2.50	2.40	2.17	2.24
VI	1.73	1.7	2.46	2.39	2.15	2.22
VII	1.73	1.71	2.44	2.39	2.13	2.19
VIII	1.73	1.71	2.45	2.42	2.15	2.2

Table 3.8. Polarization effect on atom angles with comparing basis sets (LACVP /LACVP**) for the complexes **(I-VIII)**

COMPLEX	MEASURES ANGLES(°)					
	O-Mo-O		Cl-Mo-Cl		N-Mo-N	
	LACVP	**LACVP****	**LACVP**	**LACVP****	**LACVP**	**LACVP****
I	108.03	107.07	153.94	152.72	67.56	65.84
II	154.09	106.96	107.47	152.87	67.97	66.11
III	108.02	107.08	154.25	153.00	67.68	65.99
IV	104.66	104.46	148.58	146.66	46.58	40.35
V	110.20	108.49	154.89	149.63		
VI	110.7	109.15	156.65	153.24		
VII	104.31	103.78	130.75	128.81		
VIII	109.57	108.84	157.96	156.42		

CHAPTER 4

CONCLUSION

In this study, the reaction of $MoO_2Cl_2(solv)_2$ with phenylenediamine derivatives the bidentate N-N nitrogen ligands have been examined. The novel dioxomolybdenum(VI) complexes bearing mono- and bidentate nitrogen donor ligands were prepared. All compounds exhibited monomeric structures. Both spectroscopic and computational studies confirmed that p-phenylenediamine ligands were coordinated via its one nitrogen atom. O-phenylenediamines showed a tendency to bind as bidentate ligands towards the molybdenum center. MM method fails predicting stable geometry of dioxomolybdenum containing p-phenylenediamine complexes. It was shown that DFT-B3LYP was a suitable method for geometry optimization and energy calculations of molybdenum complexes in this study. Vibrational frequency calculations for the complexes were in good agreement with the experimental values.

The novel compounds were stable in air and they had a low solubility which prevented through investigations on crystallographic studies. They can be use as potential catalysts in the olefin epoxidation reactions.

REFERENCES

Astashkin, A. V., Mader, M. L., Pacheco, A., Enemark, J. H., Raitsimring, A. M. 2000. Direct Detection of the proton-containing group coordinated to Mo(V) in the high pH form of chicken liver sulfite oxidase by refocused primary Eseem spectroscopy: structural and mechanistic implications. *J .Am. Chem. Soc*. 122: 529 –5302.

Bäckvall, J.-E. 2004. *Modern Oxidation Methods.* Wiley-VCH Ed.

Barton, C.J., .B. Jonassen and A.Weissberger, eds*.,* 1963. *In Techniques of Chemistry*. New York: Wiley-Interscience Ed.

Becke, A.D. 1993. *J. Chem. Phys*. 98: 5648

Berg, J. M., Holm, R. H. 1985. Model for the active site of oxo-transfer molybdoenzymes: synthesis, structure, and properties. *J. Am. Chem. Soc*. 107: 917-925.

Bray, R. C., Adams, B., Smith, A.T., Bennett, B., Bailey, S. 2000. Reversible dissociation of thiolate ligands from molybdenum in an enzyme of the dimethyl sulfoxide reductase family. *Biochemistry*. 39: 11258-11269.

Bregeault, J.-M. 2003. *Dalton Trans.* 3289–3302

Brito, J.A., Gomez, M., Muller, G., Teruel, H., Clinet, J.-C., Dunach, E. and Maestro, M.A.2004. *Eur. J. Inorg. Chem*. 4278–4285.

Chaudhury, P. K., Das S. K., Sarkar, S. 1996. Inhibition patterns of a model complex mimicking the reductive half-reaction of sulphite oxides. *Biochem.* J. 319: 953-959.

Das, S. K., Chaudhury, P. K., Biswas, D., Sarkar,S. 1994. Modeling for the active site of sulfite oxidase, *J. Am. Chem. Soc*. 116: 9061-9070.

Dehnicke K., Strahle J. 1981. *Angew. Chem., Int. Ed. Engl*. 20, 413

Didarul A. Chowdhury, Mohammad N. Uddin and Abul K.M. L. Rahman Chiang Mai. 2006. Synthesis and characterization of dioxo-molybdenum (VI) complexes of some dithiocarbamates. *Chiang Mai J. Sci.* 33(3) : 357 – 362

Dinda R., Sengupta, P., Mayer-Figge, H. and Sheldrick, W.S. 2002. *J. Chem. Soc. Dalton Trans.* 4434–4439.

Dowerah, D., Spence, J.T., Singh, R., Wedd, A.G., Wilson, G. L., Farchione, F., Enemark, J. H., Kristofzski, J., Bruck, M. 1987. Molybdenum(VI) and molybdenum(V) complexes with N,N'-dimethyl-N,N'-bis(2-mercaptophenyl)ethylenediamine, *J. Am. Chem. Soc*. 109: 5655- 5665.

Ellis, P. J., Conrads, T., Hille, R., Kuhn, P. 2001. Crystal structure of the 100 kDa arsenite oxidase from alcaligenes faecalis in two crystal forms at 1.64 Å and 2.03 Å, structure 9:125-132.

Enemark, J. H., Cooney, J. A, Wang, J-J., Holm, R.H. 2004. Synthetic analogues and reaction systems relevant to the molybdenum and tungsten oxotransferases, *Chem. Rev.* 104: 1175-1200.

Garner, C.D., Charnock, C.M., G. Wilkinson, R.D. Gilliard and J.A. McCleverty. 1987. *Comprehensive Coordination Chemistry*. Oxford: Pergamon Press.

Garton, S. D., Temple,C. A., Dhawan, I. K., Barber, M. J., Rajagopalan, K. V., Johnson, M.K. 2000. Resonance raman characterization of biotin sulfoxide reductase comparing oxomolybdenum enzymes in the Me_2SO reductase family. *J. Biol. Chem*. 275: 6798 – 6805.

Ge Wang, Gang Chen, Rudy L. Luck, Zhiqiang Wang, , Zhongcheng Mu, David G. Evans and Xue Duan. 2004. New molybdenum(VI) catalysts for the epoxidation of yclohexene: synthesis, reactivity and crystal structures. *Inorganica Chimica Acta*. 357:3223-3229

George, G. N., Garrett, R. M., Prince, R.C., Rajagopalan, K. V. 1996. The molybdenum site of sulfite oxidase. *J. Am. Chem. Soc*. 118: 8588-8592.

George, G. N., Hilton, J., Rajagopalan, K.V. 1996. X-ray absorption spectroscopy of dimethyl sulfoxide reductase from rhodobacter sphaeroides. *J. Am. Chem. Soc*. 118:1113-1117.

George, G. N., Hilton, J., Temple, C., Prince, R. C., Rajagopalan, K. V. 1999. Structure of the molybdenum site of dimethyl sulfoxide reductase. J. *Am. Chem. Soc.* 121: 1256-1266.

George, G. N., Kipke, C. A., Prince, R. C., Suede, R. A., Enemark, J. H., Cramer, S. P. 1989. Structure of the active site of sulfite oxidase, x-ray absorption spectroscopy of the molybdenum (IV), molybdenum(V), and molybdenum(VI) oxidation states, *Biochemistry* 28: 5075- 5080.

Gnecco, J.A., Borda, G. and Reyes, P. 2004. Catalytic epoxidation of cyclohexene using Molybdenum complexes. *Journal of the Chilean Chemical Society*. 49:179-184

Gonçalves, I.S., Santos, M.A, Romão, C.C., Lopes, A.D., Rodríguez-Borges, J.E, Pillinger, M., Ferreira, P., Rocha, J. and Kühn, F.E. 2001. Chiral dioxomolybdenum(VI) complexes for enantioselective alkene epoxidation. *Journal of Organometallic Chemistry.* 626: 1-10

Hall, P. Basu. 2006. *Chem. Eur. J*. 12: 7501.

Harwood, L.M., Moody, C.J. 1989. *Experimental Organic Chemistry*. Oxford University Press.

Hay, P.J. and Wadt, W.R. 1985. *J. Chem. Phys*. 82: 270-284-299.

Hille, R. 1996. Structure and function of mononuclear molybdenum enzymes, *J. Biol. Inorg.* Chem. 1: 397-404.

Hille, R. 1996. The mononuclear molybdenum enzymes. *Chem. Rev*. 96: 2757-2816.

Hille, R. 2002. Molybdenum and tungsten in biology. *Trends in Biochemical Science.* 27: 360-367.

Holm, R. H. 1987. Metal-centered oxygen atom transfer reactions. *Chem. Rev.* 87: 1401-1449.

Holm, R. H**.** 1990. The biologically relevant oxygen atom transfer chemistry of molybdenum: from synthetic analogue systems to enzyme. *Coord. Chem. Rev.* 100 : 183-221.

Holm, R. H. 1996. Structural and functional aspects of metal sites in biology. *Chem. Rev.* 96 : 2239-2314.

Holm, R.H. 1990. *Coord. Chem. Rev.* 100 : 183–221.

Holm, R.H., Kennepohl, P. and Solomon, E.I. 1996. *Chem. Rev.* 96: 2239–2314.

Jorgensen, K.A. 1989. *Chem. Rev.* 89 : 431–458.

Jurisson, S. 1997. *Inorganic Synthesis.* 31: 246-247

Kail, B.W, Pe´rez, L.M, Zaric´, S.D., Millar, A.J.,Young, C.G., Basu, M.B., Stolz, P., Smith, M. T. 2003. A coordination chemist's view of the active sites of mononuclear molybdenum enzymes. *Current Science.* 84: 1412-1418.

Kisker, C., Schindelin, H., Pacheco, A., Wehbi, W. A., Garrett, R. M., Rajagopalan, K. V., Enemark, J. H., Rees, D. C. 1997. Molecular basis of sulfite oxidase deficiency from the structure of sulfite oxidase. *Cell*. 91: 973-983.

Kisker, C., Schindelin, H., Rees, D. C. 1997. Molybdenum-cofactor-containing enzymes: structure and mechanism, *Annu. Rev. Biochem.* 66: 233-267.

Krishnan, R., Binkley, J.S., Seeger, R., Pople, J.A. 1980. *J. Chem. Phys*. 72:650.

Kühn, F.E, Lopes, A.D, Santos, A., Herdtweck, E., Haider, J.J., Romão C.C. and Santos, A.G. 2000. Lewis base adducts of bis-(halogeno)dioxomolybdenum(VI): syntheses, structures, and catalytic applications *Journal of Molecular Catalysis*. 151:147-160.

Kühn, F.E., Herdtweck, E., Haider, J.J, Herrmann, W.A., Gonçalves, I.S, Lopes, A.D. and Romão, C.C. 1999. Bis-acetonitrile(dibromo)dioxomolybdenum(VI) and derivatives: synthesis, reactivity, structures and catalytic applications. *Journal of Organometallic Chemistry* 583: 3-10

Kühn, F.E., Santos, M.A, Gonçalves, I.S., Romao, C.C, Lopes, A.D. 2001. *Appl. Organomet Chem*. 43: 15.

Kumar S.B., Chaudhury, M. 1991. *J. Chem. Soc. Dalton Trans.*2169.

Laughlin, L. J., Young, C. G. 1996. Oxygen atom transfer, coupled electron-proton transfer, and correlated electron-nucleophile transfer reactions of oxomolybdenum(IV) and dioxomolybdenum(VI) complexes. *Inorg. Chem*. 35: 1050-1958.

Leonard, J., Lygo, B., Procter, G. 1995. *Advanced pratical organic chemistry*. Blackie Academic and Professional, an imprint of Chapman and Hall publishers.

Li, H.-K., Temple, C., Rajagopalan, K.V., Schindelin, H. 2000; The 1.3 Å crystal structure of rhodobacter sphaeroides dimethyl sulfoxide reductase reveals two distinct molybdenum coordination environments *J. Am. Chem. Soc.* 122:7673-7680.

Lim, B. S., Holm, R. H. 2001. Bis(dithiolene)molybdenum analogues relevant to the DMSO reductase enzyme family: synthesis, structures, and oxygen atom transfer reactions and kinetics, *J. Am. Chem. Soc*. 123: 1920-1930.

Lorber, C., Plutino, M. R., Elding, L. I., Nordlander, E. 1997. Kinetics of oxygen-atom transfer reactions involving molybdenum dithiolene complexes. *J. Chem. Soc., Dalton Trans*, 3997-4003.

Lorber, C.Y, Smidt S.P, and Osborn, J.A. 2000. *Eur. J. Inorg. Chem.* 655–658

Luís F. Veiros, Ângela Prazeres, Paulo J. Costa, Carlos C. Romão, Fritz E. Kühn and Maria José Calhorda. 2006. Olefin epoxidation with tert-butyl hydroperoxide catalyzed by MoO_2X_2L complexes: a DFT mechanistic study. *Dalton Trans.* 1383–1389.

McAlpine, A. S., McEwan, A. G., Bailey, S. 1998. The high resolution crystal structure of DMSO reductase in complex with DMSO, *J. Mol. Biol*. 275: 613-623.

McAlpine, A. S., McEwan, A. G., Shaw, A. L., Bailey, S. 1997. Molybdenum active centre of DMSO reductase from rhodobacter capsulatus, J. Biol. Inorg. Chem. 2: 690-701

McCleverty, J.A., Denti, G. and Reynolds, S. 1983. *J. Chem. Soc.*, *Dalton Trans*. 81-89.

McLean, A.D., Chandler, G.S. 1980. *J. Chem. Phys*. 72: 5639.

Meister, G.E. and Butler, A. 1994. *Inorg. Chem.* 33: 3269–3275

Meunier, B. 2000. *Metal-oxo and metal-peroxo species in catalytic oxidations*, Berlin: Springer.

Palanca P., Picher T., Sanz V., Go'mez P., Romero, Llopis E., Domenech A., Cervilla, A.

1990. *J. Chem. Soc. Chem. Comm.* 531.

Rajagopalan, K. V. 1991. The pterin molybdenum cofactors. *Adv. Enzymol*. 64: 215−290.

Rao, S.N., Munshi K.N., Rao, N.N. 2000. Reactivity of -Benzoin Oxime with Molybdenum(VI). *J. Mol. Cat. A: Chem.* 156 : 205–211.

Reynolds, M.S., Babinski, K.J., Bouteneff, M.C., Brown, J.L., Campbell, R.E., Cowan, M.A., Durwin, M.R., Foss, T., O'Brien P. and Penn, H.R. 1997. *Inorg. Chim. Acta.* 263: 225–230

Schultz, B. E., Gheller, S. F., Muetterties M. C., Scott, M. C., Holm, R. H. 1993. Molybdenum mediated oxygen-atom transfer: an improved analog reaction system of the molybdenum oxotransferases. *J. Am. Chem. Soc*. 115: 2714-2722.

Schultz,B. E., Hille,R., Holm, R. H. 1995. Direct OAT in the mechanism of action of rhodobacter sphaeroides dimethyl sulfoxide reductase, *J. Am. Chem. Soc.* 117: 827-828.

Sellmann, D., Hadawi, B., Knoch F., and Mool, M. 1995. Transition-metal complexes with sulfur ligands. Syntheses, X-ray Crystal Structures, and Reactivity of Molybdenum(II) Complexes with Thioetherthiolate Ligands Having XS4 Donor Atom Sets (X=S,O,NH). *Inorg.Chem.* 34: 5963

Shriver, D.F. 1969. *The Manipulation of Air Sensitive Compounds*. New York: McGraw-Hill.

Sigel, A., Sigel, H. 2002 *Molybdenum and tungsten -their roles in biological processes.* Newyork: Marcell Decker

Sugimoto, H., Harihara, M., Shiro, M., Sugimoto, K., Tanaka, K., Miyake, H., Tsukube, H. 2005. Dioxo-molybdenum(VI) and mono-oxo-molybdenum(IV) complexes supported by new aliphatic dithiolene ligands: new models with weakened modo bond characters for the arsenite oxidase active site. *Inorg. Chem*. 44: 6386-6392.

Thapper, A., Deeth, R. J., Nordlander, E., 2002. A density functional study of oxygen atom transfer reactions between biological oxygen atom donors and molybdenum(IV) bis(dithiolene) complexes. *Inorg. Chem*. 42: 6695–6702.

Tong, Y.-L., Ma, J.-F., Law, W.-F., Yan, Y., Wong, W.-T., Zhang, Z.-Y., Mak, T. C. W., Ng, D. K. P. 1999. Synthesis, electrochemistry, and oxygen-atom transfer reactions of dioxotungsten(VI) and -molybdenum(VI) complexes with N_2O_2 and N_2S_2 tetradentate ligands, Eur. *J. Inorg. Chem*. 313-321.

Tong, Y.-L., Yan, Y., Chan, E. S. H., Yang, Q., Mak, T. C. W., Ng, D. K. P. 1998. Cis-dioxo-tungsten(VI) and -molybdenum(VI) complexes with N_2O_2 tetradentate ligands: synthesis, structure, electrochemistry and oxo-transfer properties *J. Chem. Soc., Dalton Trans*. 3057-3064.

Tucci, G. C., Donahue, J. P., Holm, R. H. 1998. Comparative kinetics of oxo transfer to substrate mediated by bis(dithiolene)dioxomolybdenum and -tungsten complexes. *Inorg. Chem*. 37: 1602-1608

Tuczek, F., Horn, K.H., Lehnert, N. 2003. Vibrational spectroscopic properties of molybdenum and tungsten N_2 and N_2H_x complexes with depe coligands: comparison to dppe systems and influence of H-bridges. *Coordination Chemistry Reviews*. 245: 107–120

Ueyama, N., Oku, H., Kondo, M., Okamura, T., Yoshinaga, N., Nakamura, A. 1996. Trans influence of oxo and dithiolene coordination in oxidized models of molybdenum oxido- reductase. *Inorg. Chem.* 35: 643-650.

Vlcˇek A.Jr. 2002. Coord. Chem. Rev. 230: 225

Warren J.H. 2003 *A guide to molecular mechanics and quantum chemical calculations* Wavefunction Inc.

Webster, C.E, Hall, M.B. 2001. *J. Am. Chem. Soc*. 123: 5820

Wilshire, J.P., Leon, L., Bosserman, P., Sawyer, D.T. 1979. *J. Am. Chem. Soc*. 101

Young, C. G., Laughlin, L. J.,Colmane, S., Scrofani, S. D. B. 1996. Oxygen atom transfer, sulfur atom transfer, and correlated electron-nucleophile transfer reactions of oxo- and thiomolybdenum(IV) complexe. *Inorg. Chem*. 35: 5368-5377.

Z'miric´, A., Zaric´, S.D. 2002, *Inorg. Chem. Commun*. 5: 446.

Zaric, S., Hall, M.B. 1997. *Molecular modeling and dynamics of bioinorganic systems.* Kluwer Academic Publishers.

Zekri O., Boutamine, S., Hank, Z., Slaouti, H., Meklati M. and Vittori, O. 2000. *Synth. React. Inorg. Met-Org. Chem.* 30: 2009-2028

APPENDIX A

^{1}H NMR, ^{13}C NMR OF THE PRODUCTS

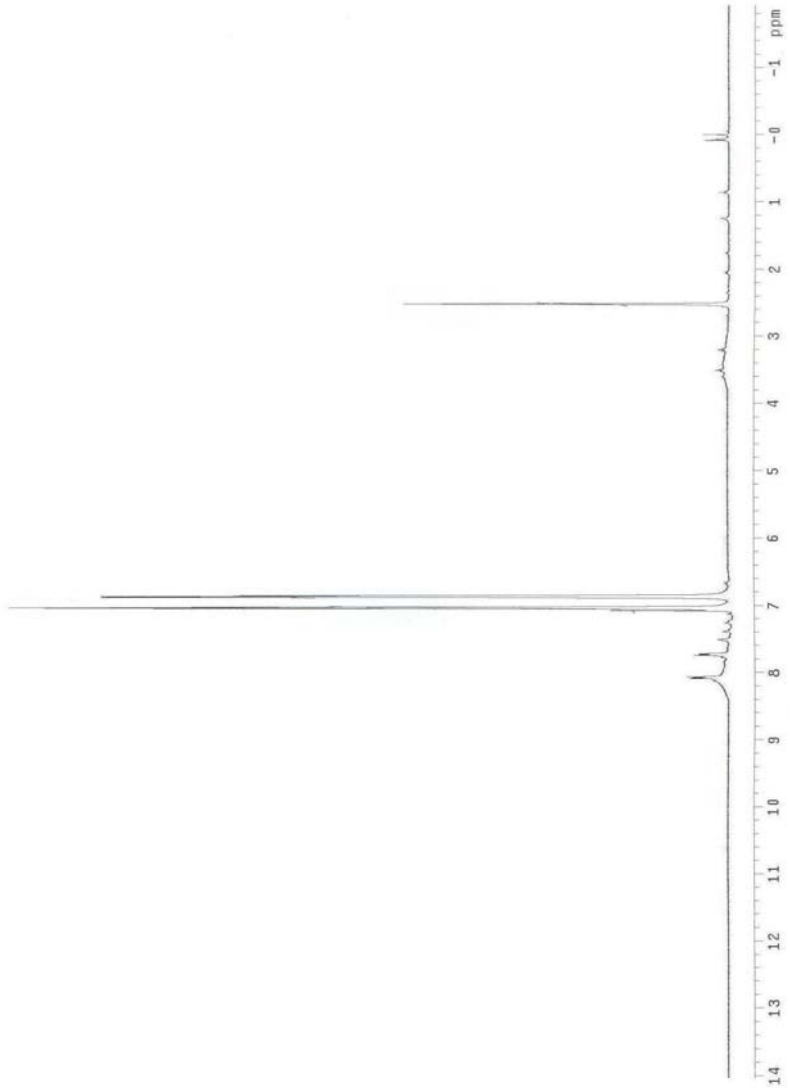

Figure A.1. ^{1}H-NMR spectrum of $[MoO_2Cl_2((HN)_2C_6H_4)]$ **(I)**

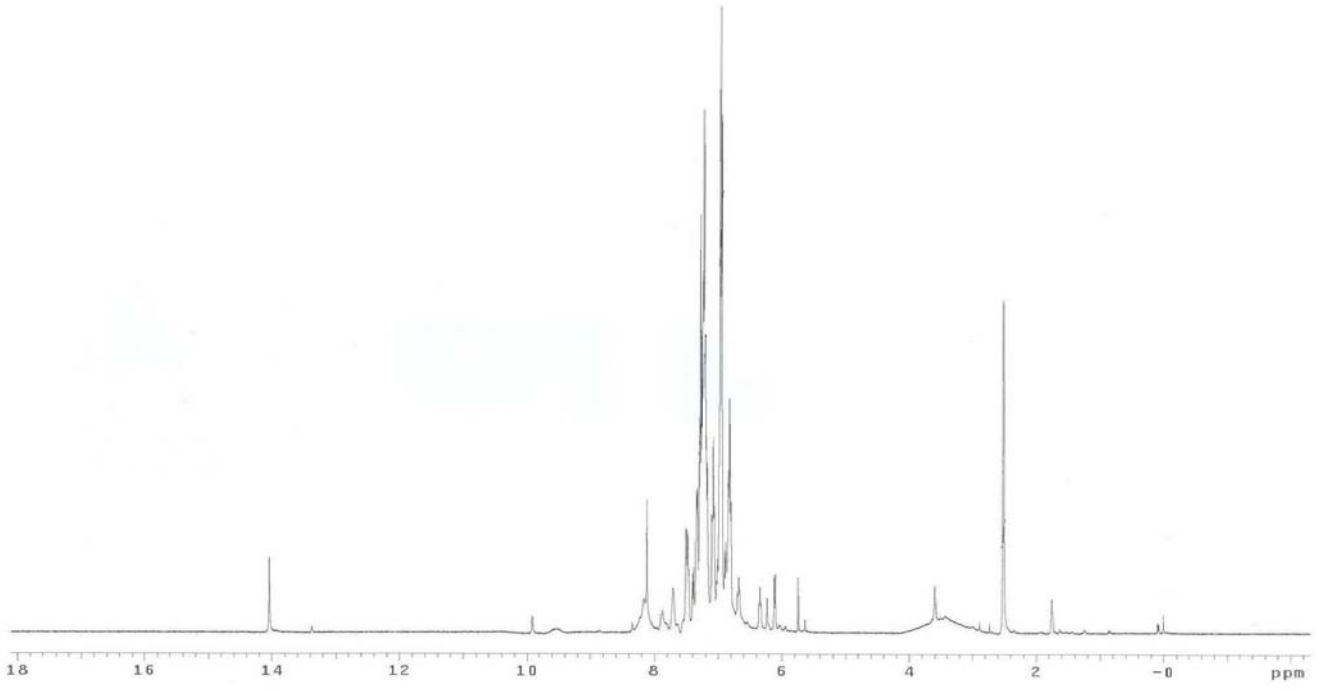

Figıre A.2. ^{1}H-NMR spectrum of $[MoO_2Cl_2\ ((HN)(HNC_6H_5)C_6H_4)]$ **(II)**

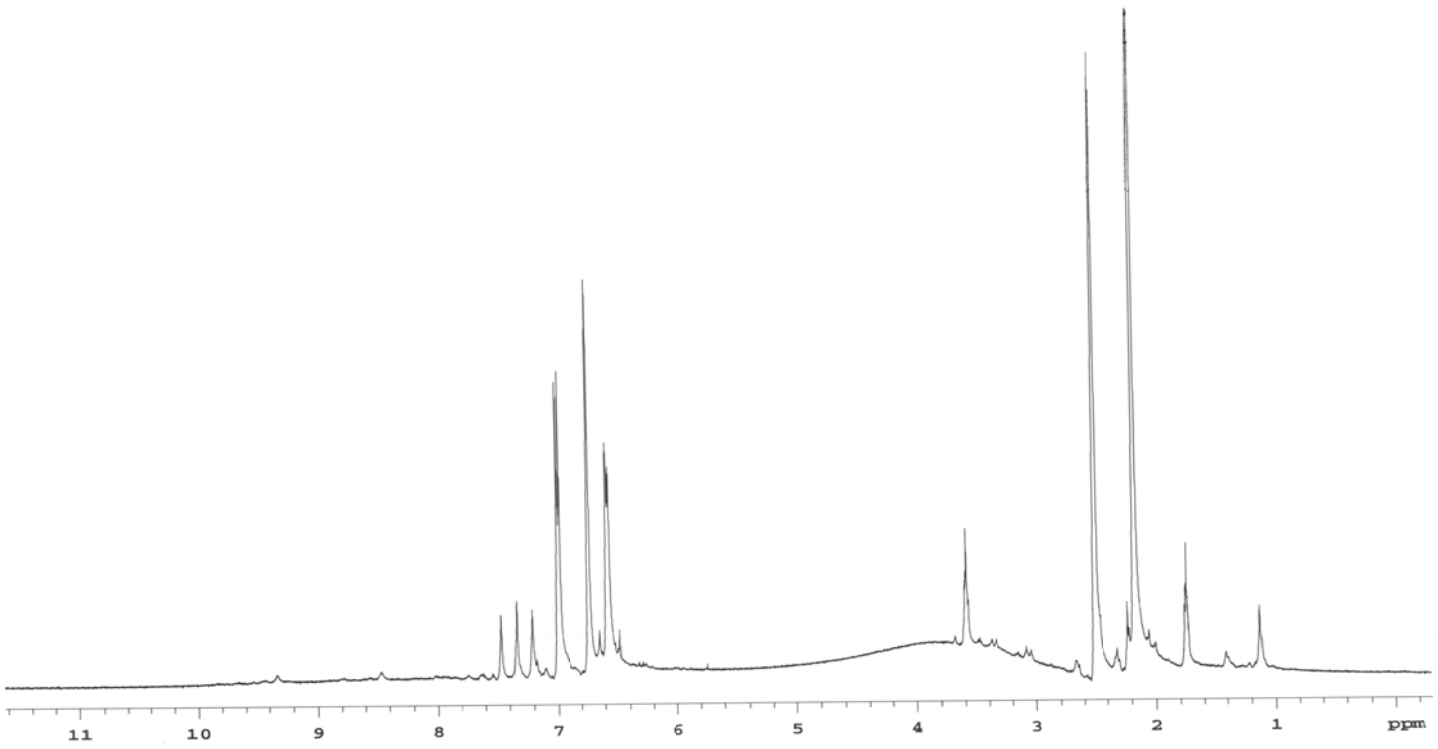

Figure A.3. ^{1}H NMR spectrum of $[MoO_2Cl_2(HN)_2C_6H_5(CH_3)]$ **(III)**

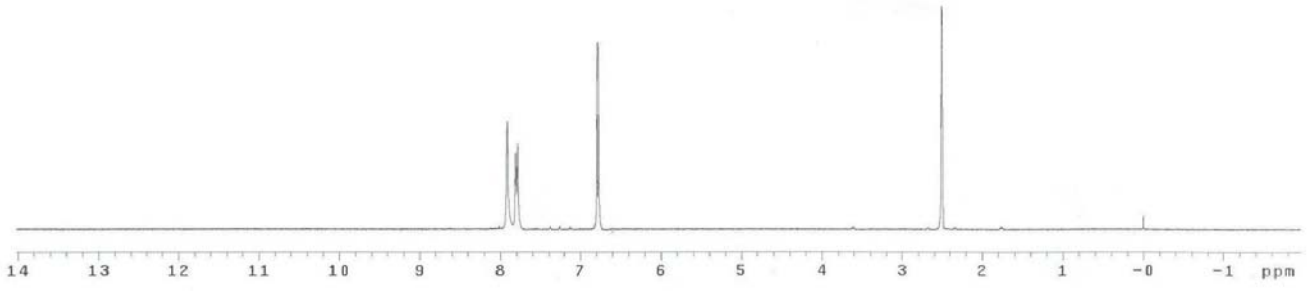

Figure A.4. ^{1}H-NMR spectrum of $[MoO_2Cl_2(N_2C_6H_3(NO_2))]$ **(IV)**

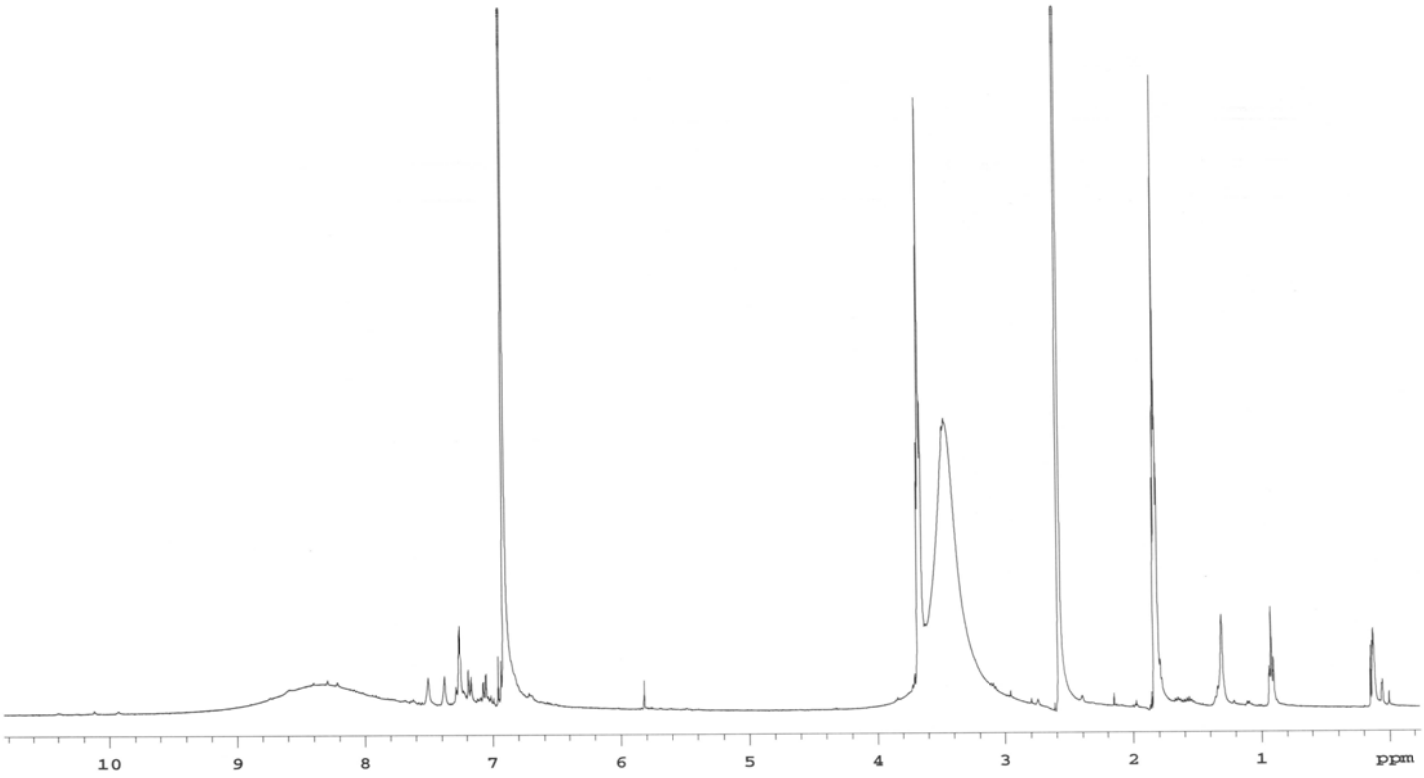

Figure A.5. ^{1}H-NMR spectrum of $[MoO_2Cl_2((HN)_2C_6H_4)]$ **(V)**

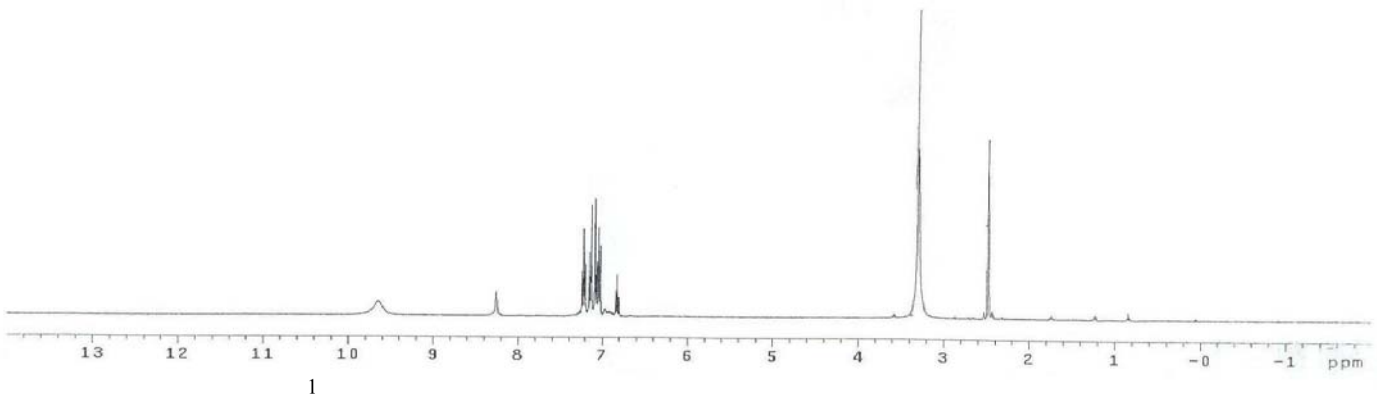

Figure A.6. ^{1}H-NMR spectrum of $[MoO_2Cl_2((HN)(HNC_6H_5)C_6H_4)]$ **(VI)**

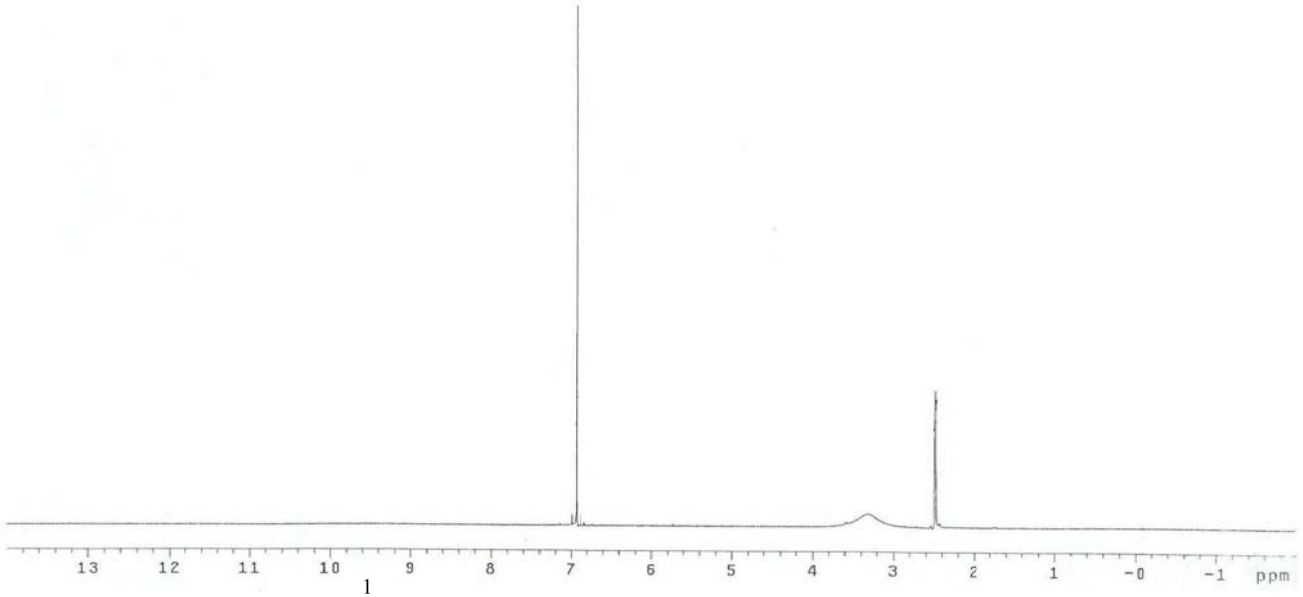

Figure A.7. ^{1}H-NMR spectrum of $[MoO_2Cl_2((H_2N)C_6H_2Cl_2)]$ **(VII)**

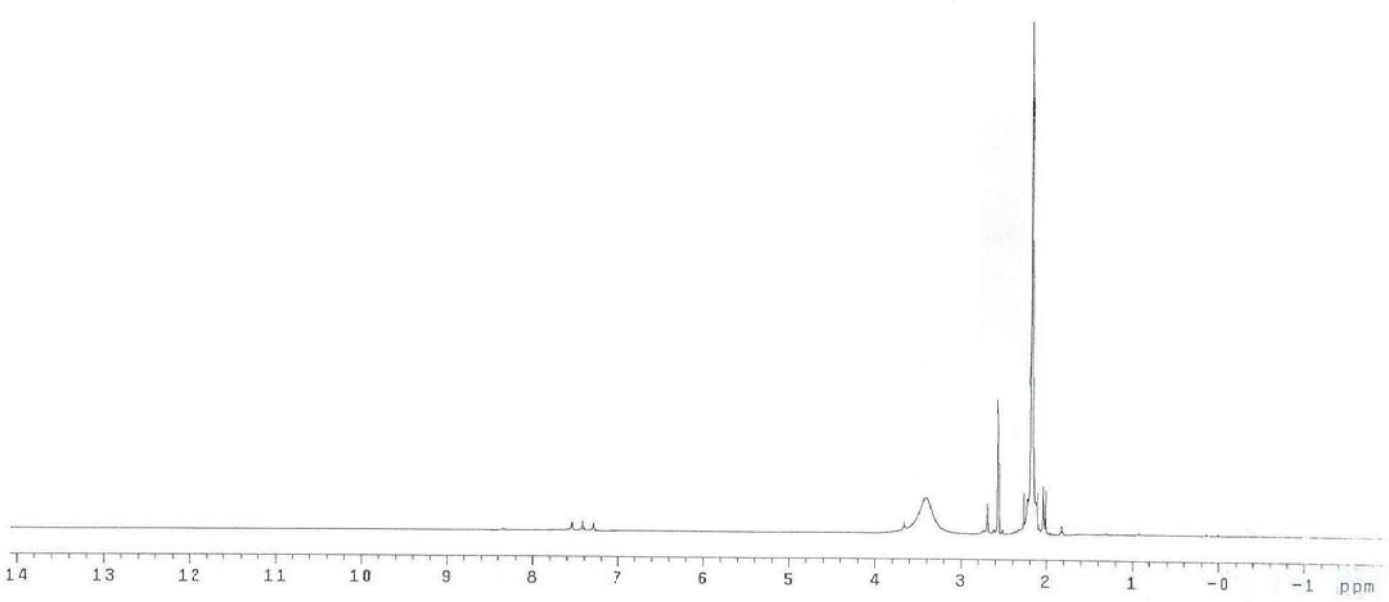

Figure A.8. ^{1}H-NMR spectrum of $[MoO_2Cl_2(HNNH_2C_6(CH_3)_4)]$ **(VIII)**

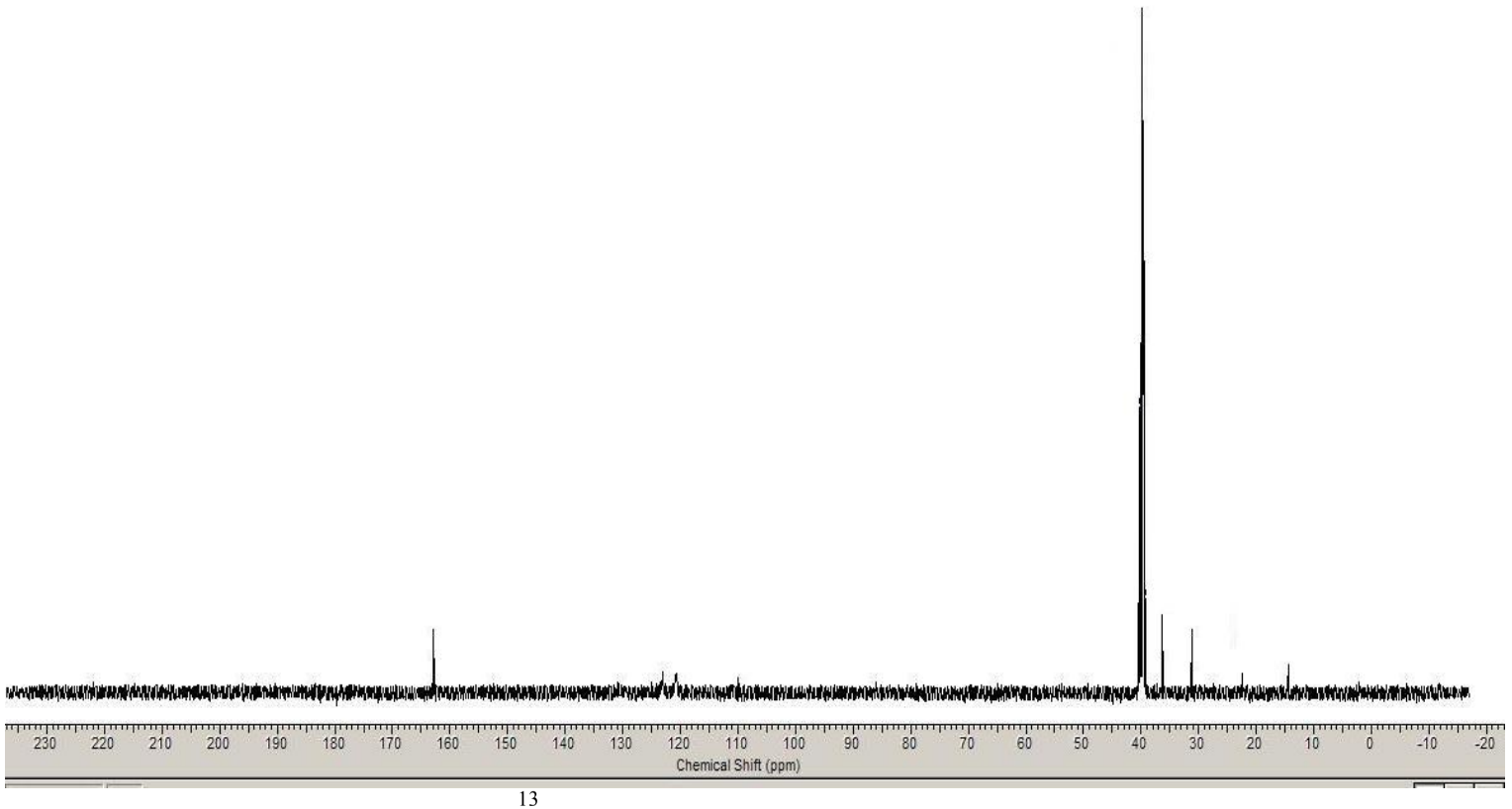

Figure A.9. ^{13}C-NMR spectrum of $[MoO_2Cl_2((HN)_2C_6H_4)]$ **(I)**

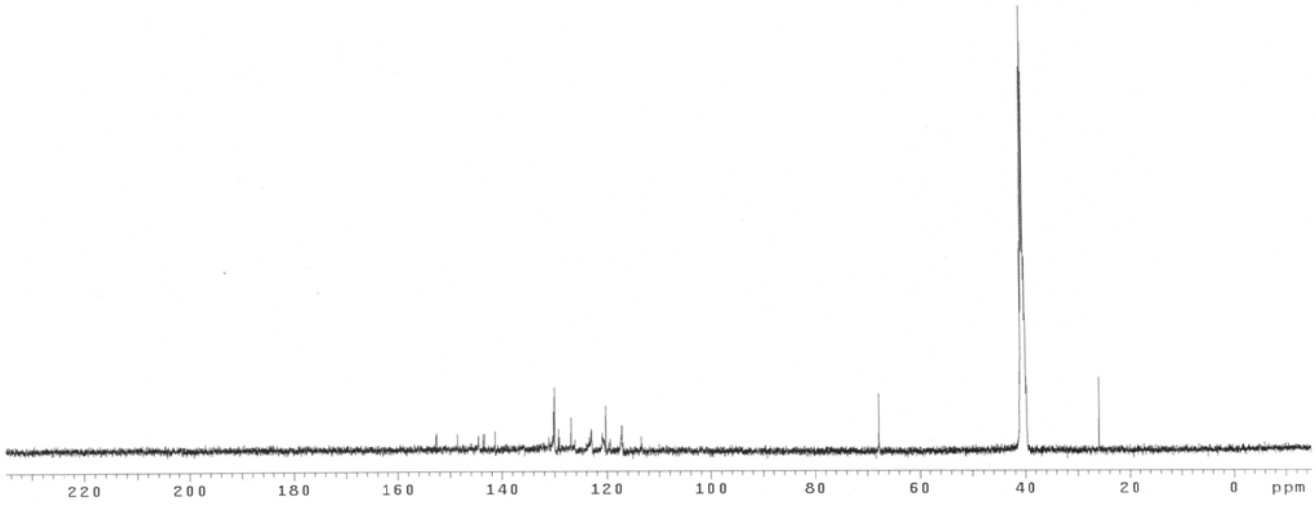

Figure A.10. ^{13}C-NMR spectrum of $[MoO_2Cl_2((HN)(HNC_6H_5)C_6H_4)]$ **(II)**

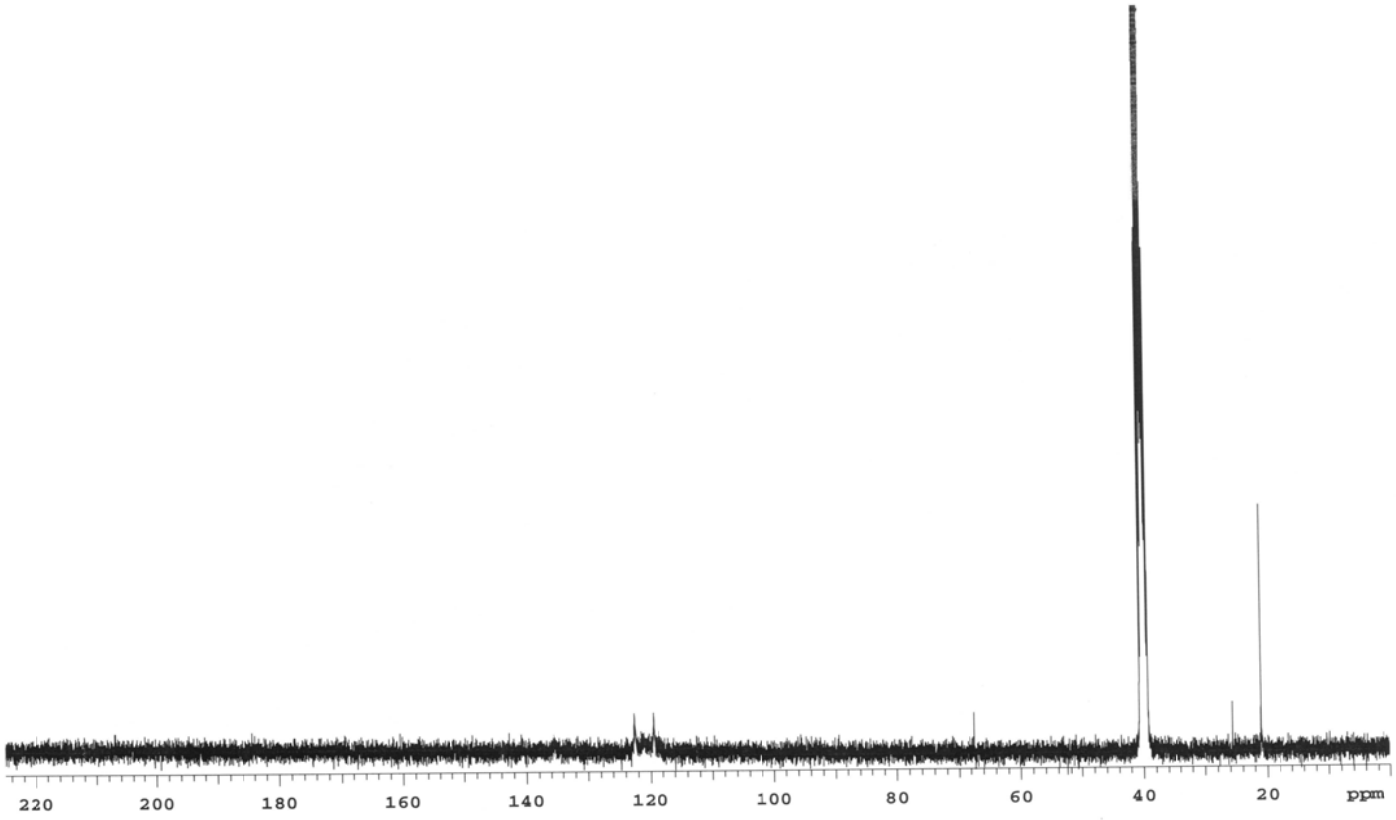

Figure A.11. ^{13}C-NMR spectrum of $[MoO_2Cl_2((HN)_2C_6H_5(CH_3))]$ **(III)**

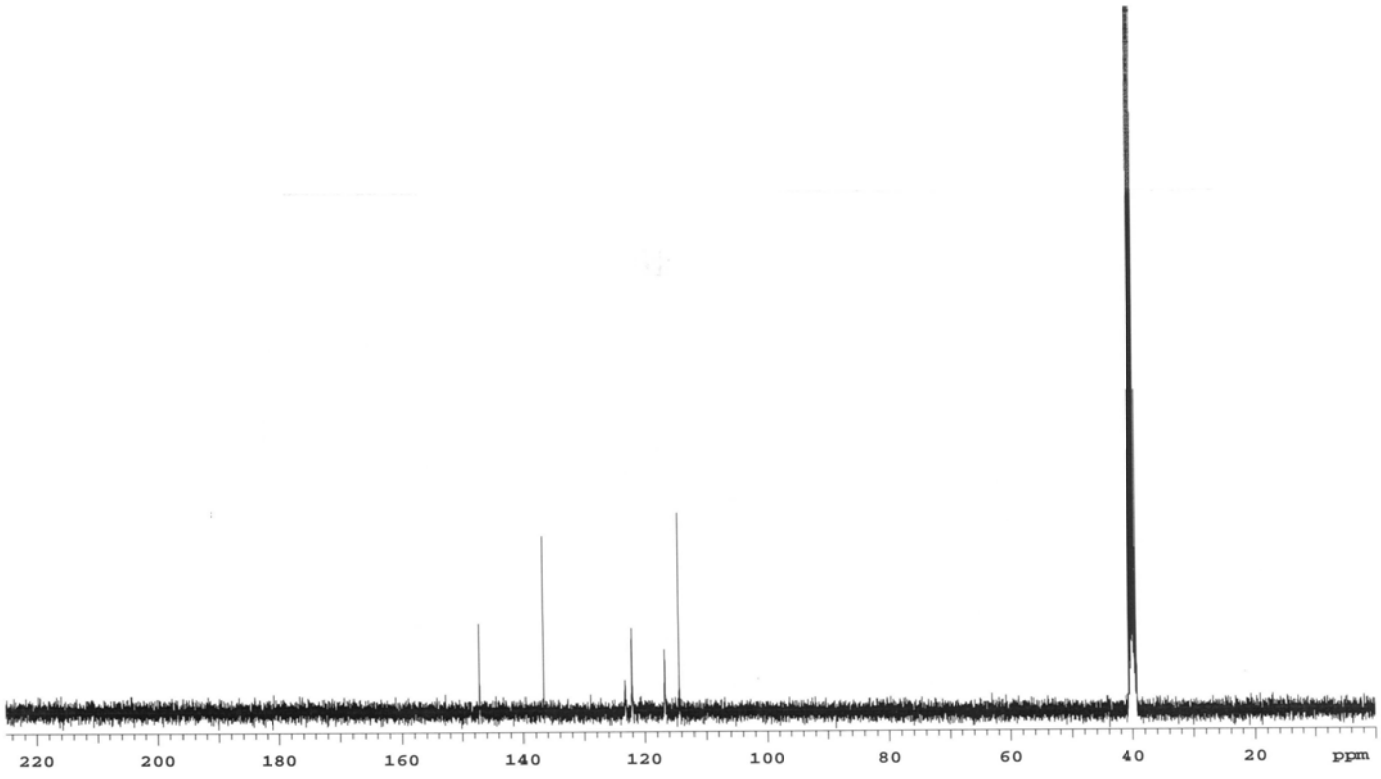

Figure A.12. ^{13}C-NMR spectrum of $[MoO_2Cl_2(N_2C_6H_3(NO_2))]$ **(IV)**

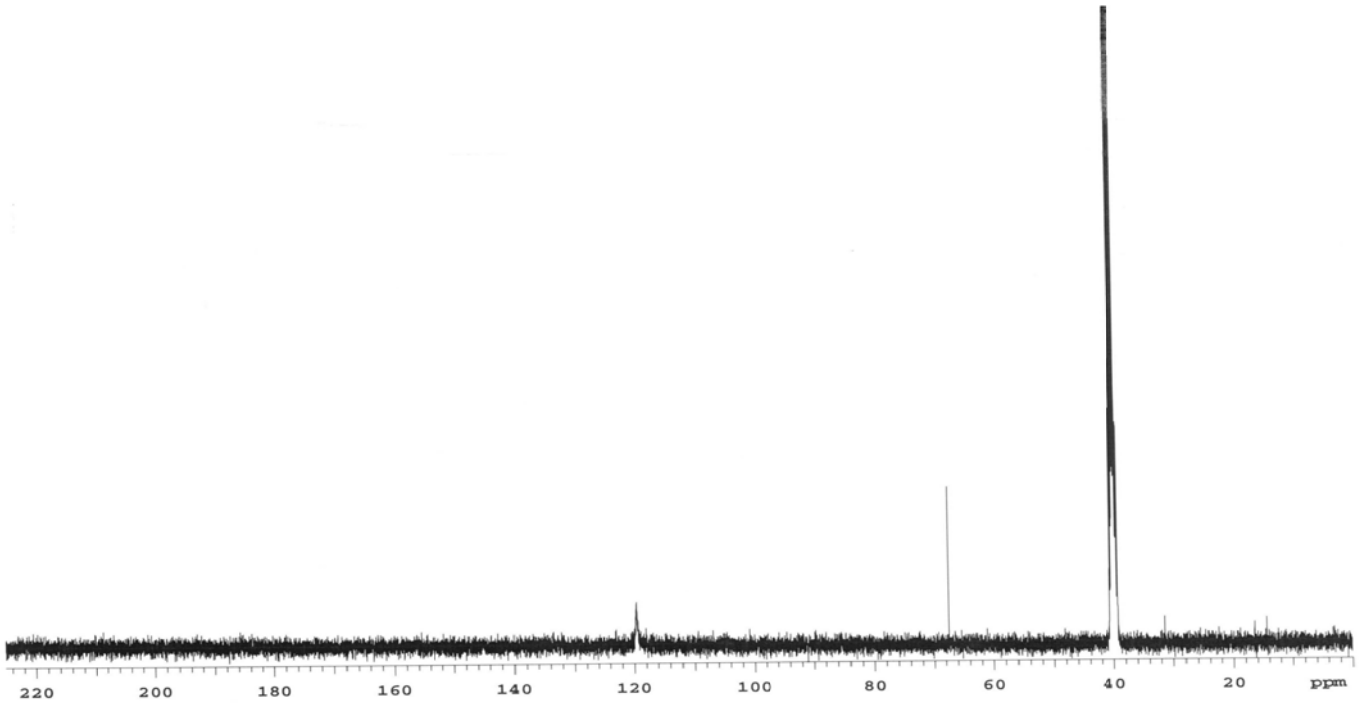

Figure A.13. ^{13}C-NMR spectrum of $[MoO_2Cl_2((HN)_2C_6H_4)]$ **(V)**

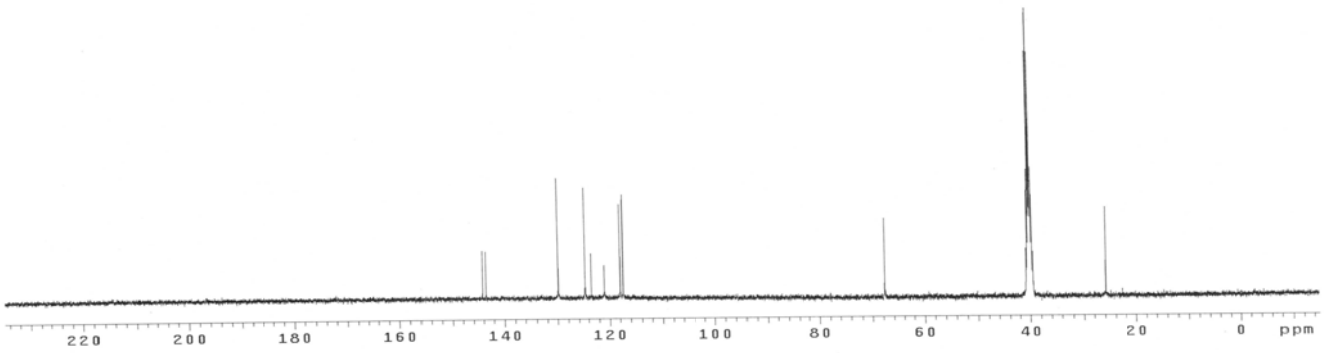

Figure A.14. ^{13}C-NMR spectrum of $[MoO_2Cl_2((HN)(HNC_6H_5)C_6H_4)]$ **(VI)**

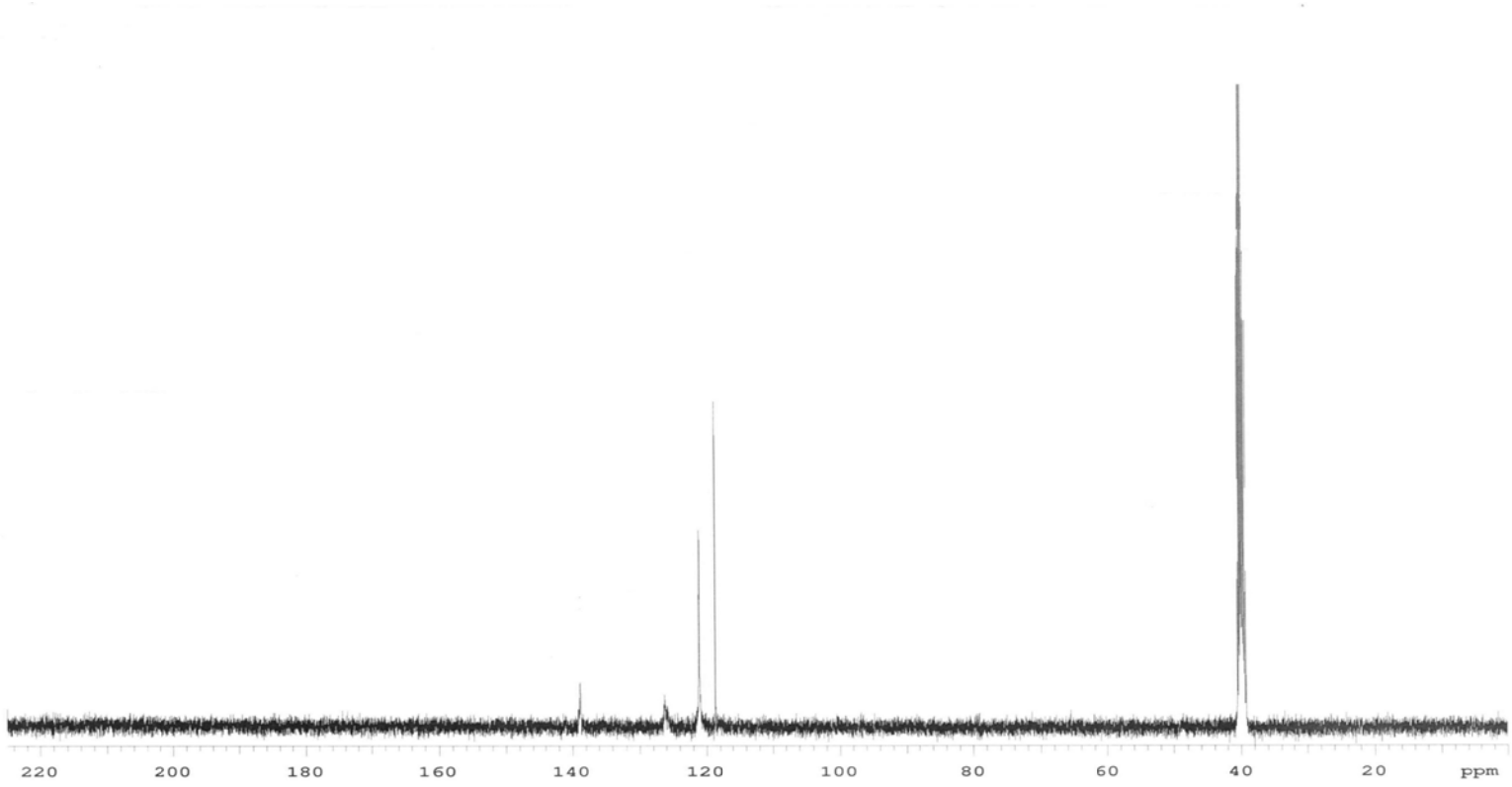

Figure A.15. ^{13}C-NMR spectrum of $[MoO_2Cl_2((H_2N)C_6H_2Cl_2)]$ **(VII)**

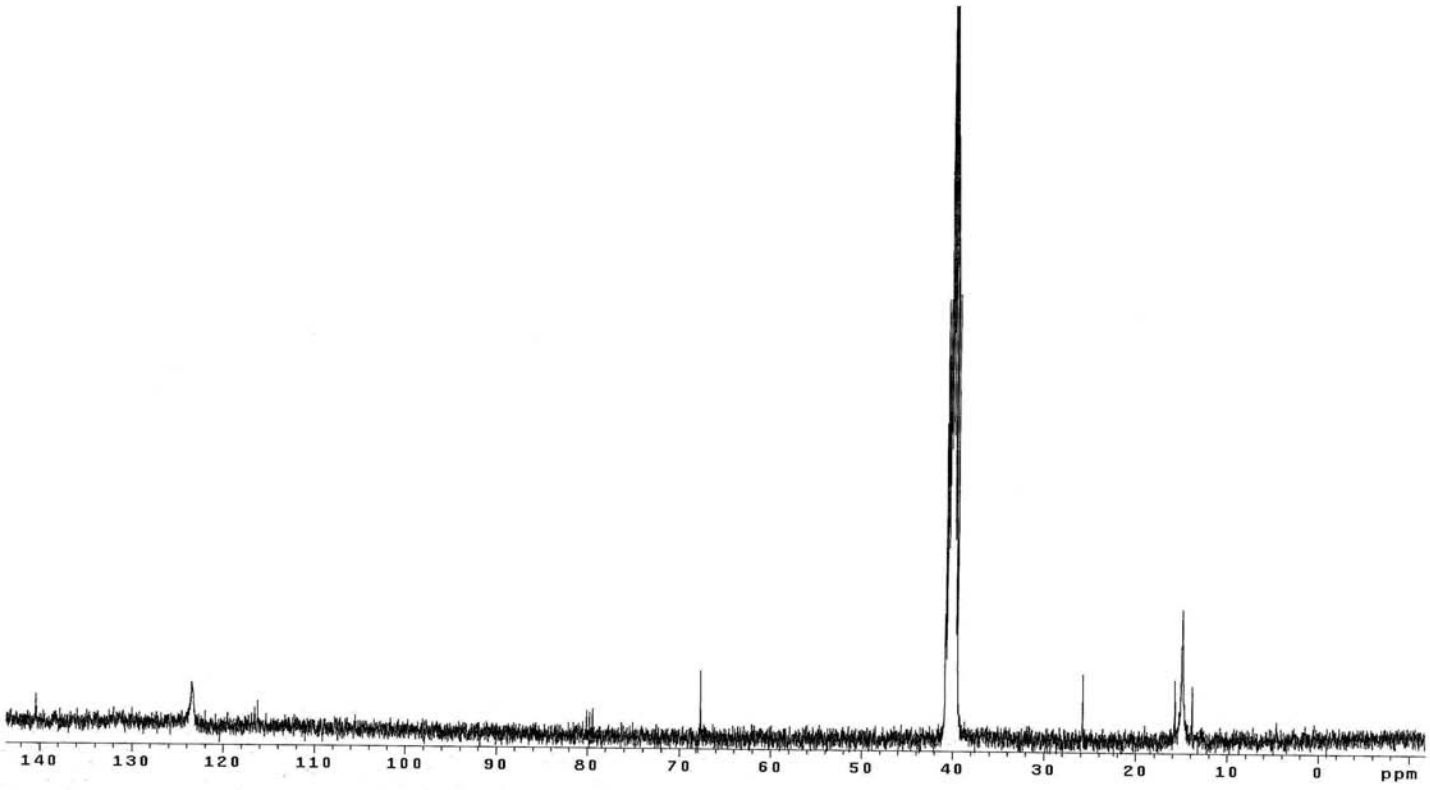

Figure A.16. ^{13}C-NMR spectrum of $[MoO_2Cl_2(HNNH_2C_6(CH_3)_4)]$ **(VIII)**

APPENDIX B

FT-IR SPECTRUMS OF THE PRODUCTS

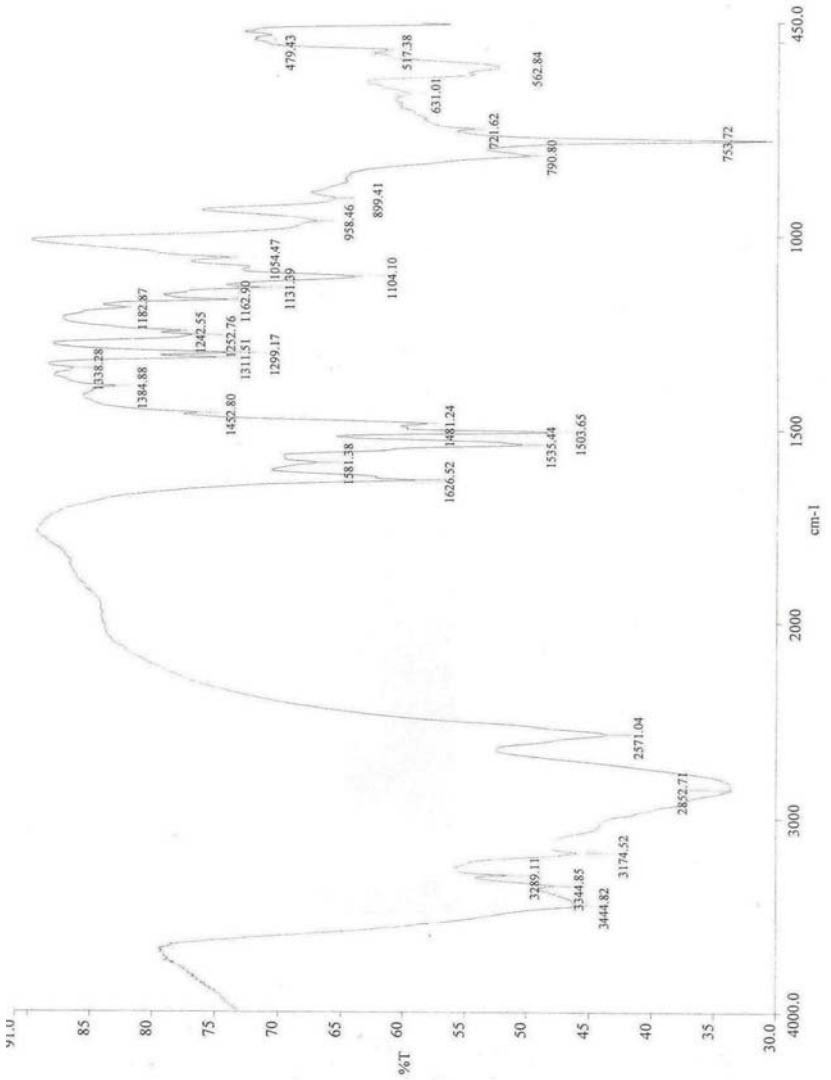

Figure B.1. FT-IR spectrum of $[MoO_2Cl_2((HN)_2C_6H_4)]$ **(I)**

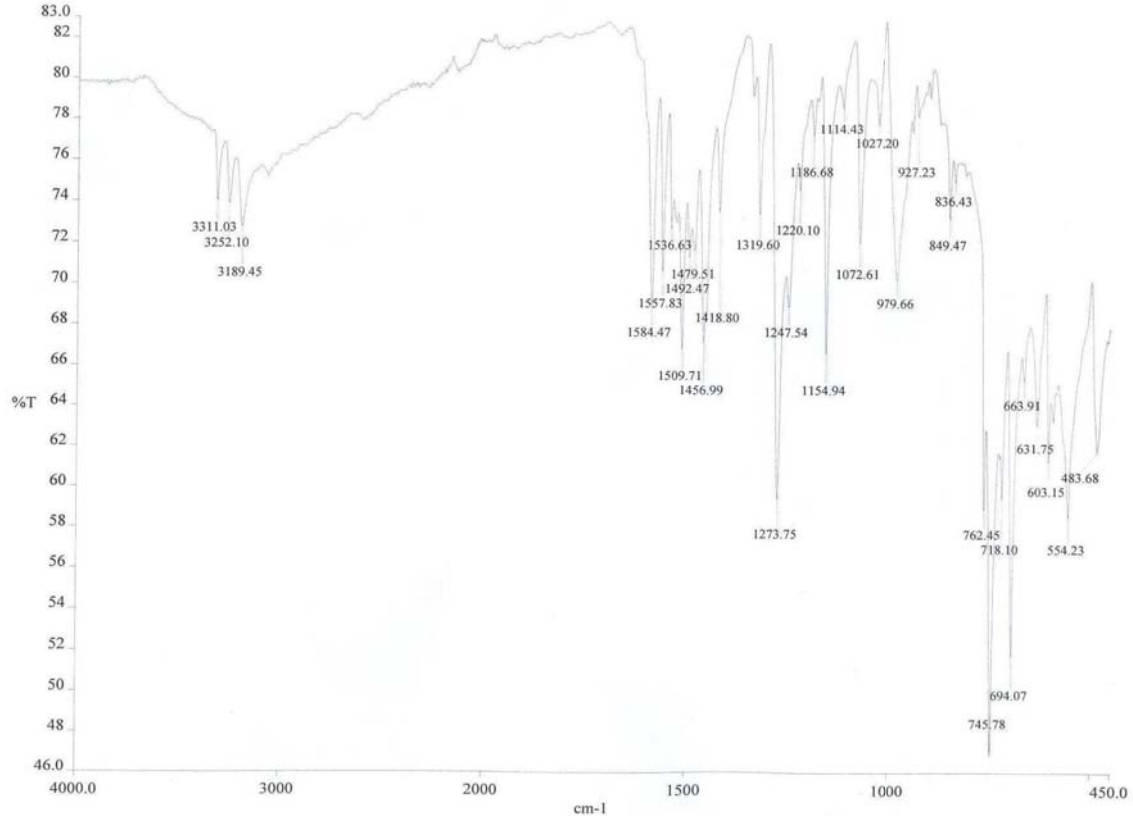

Figure B.2. FT-IR spectrum of $[MoO_2Cl_2((HN)(HNC_6H_5)C_6H_4)]$ **(II)**

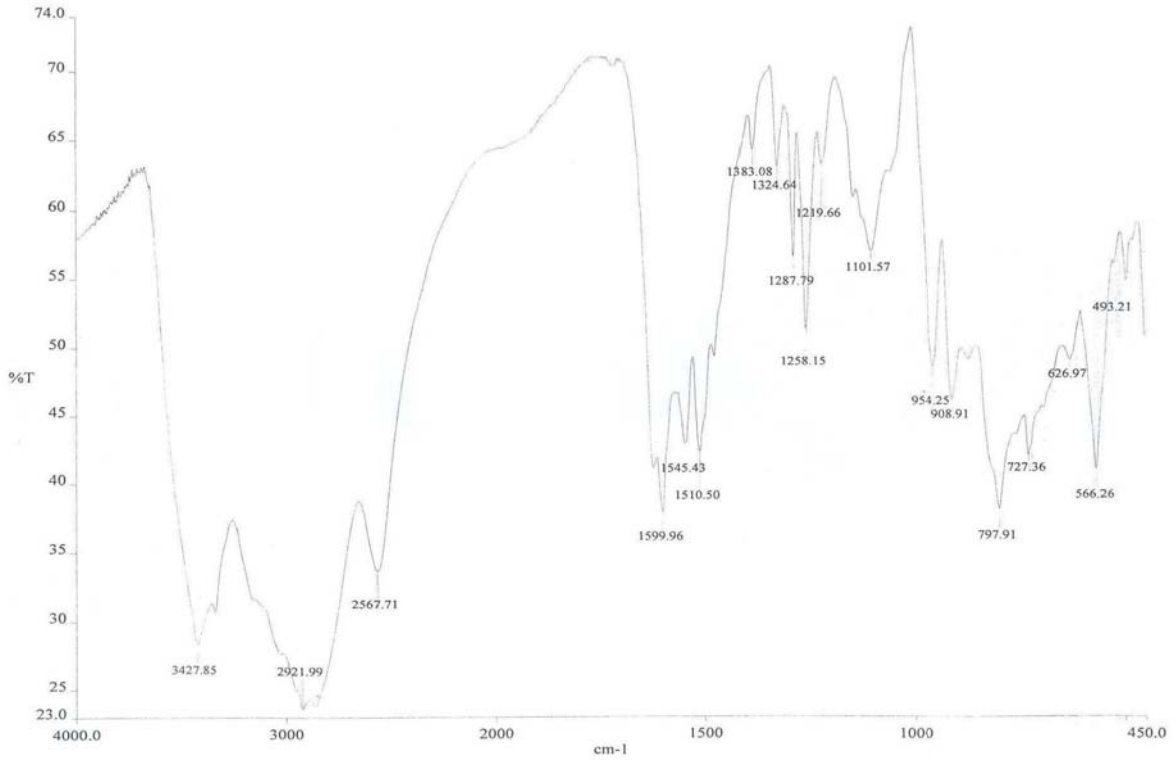

Figure B.3. FT-IR spectrum of $[MoO_2Cl_2((HN)_2C_6H_5(CH_3))]$ **(III)**

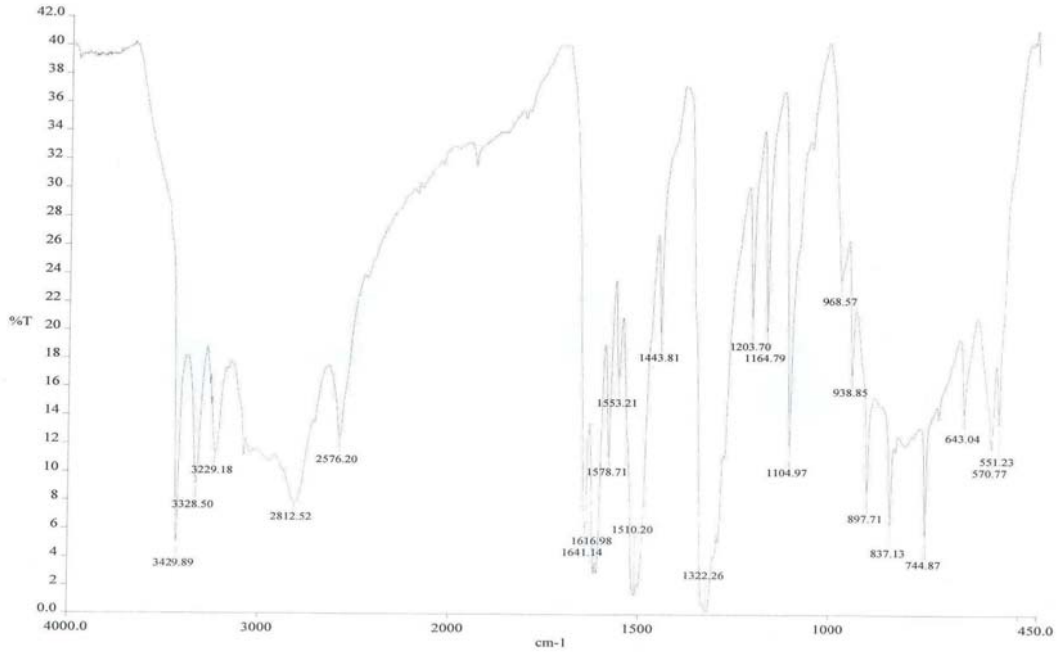

Figure B.4. FT-IR spectrum of $[MoO_2Cl_2(N_2C_6H_3(NO_2))]$ **(IV)**

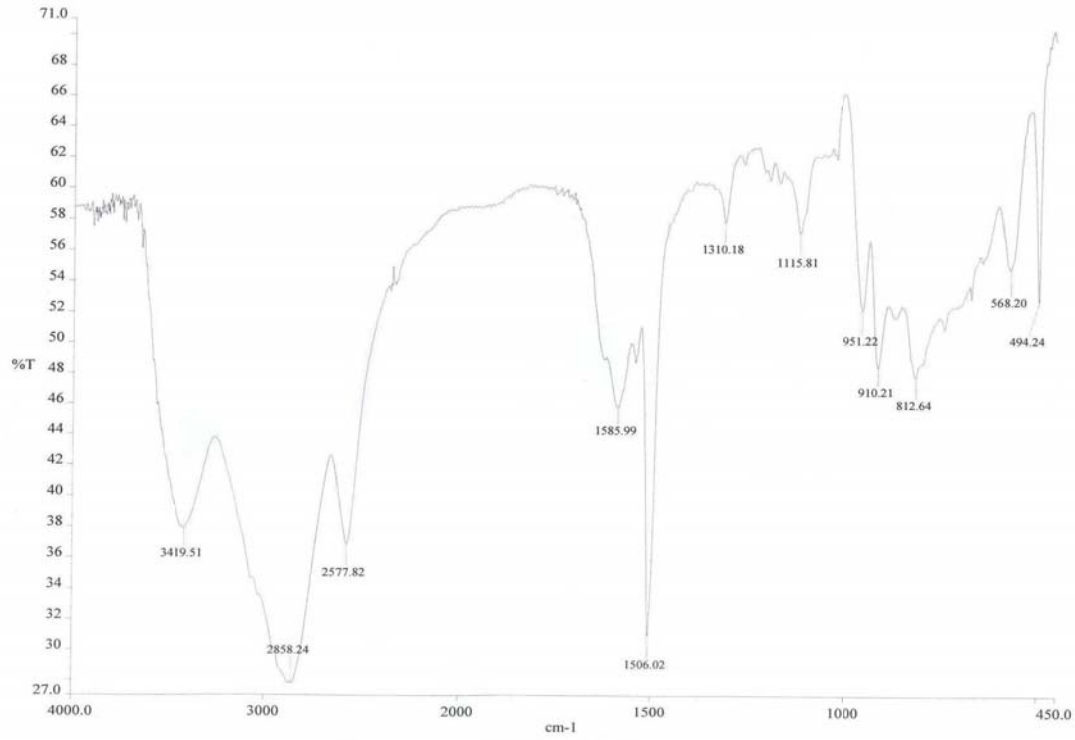

Figure B.5. FT-IR spectrum of $[MoO_2Cl_2((HN)_2C_6H_4)]$ **(V)**

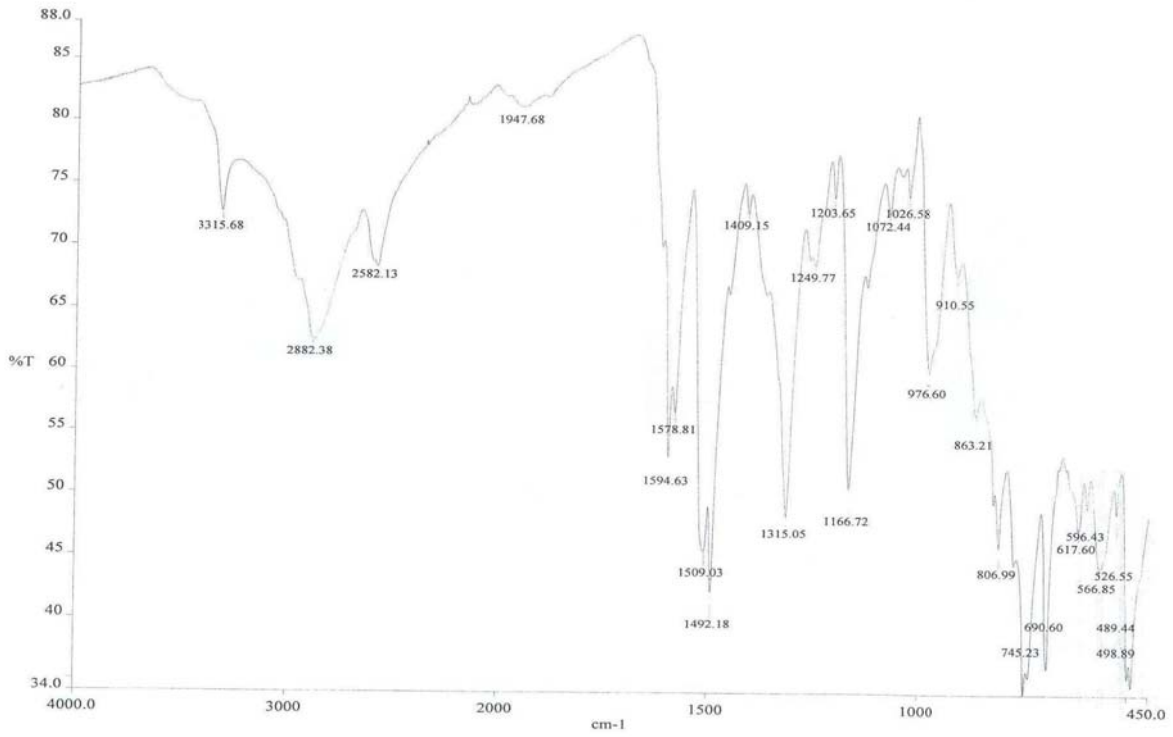

Figure B.6**.** FT-IR spectrum of $[MoO_2Cl_2((HN)(HNC_6H_5)C_6H_4)]$ **(VI)**

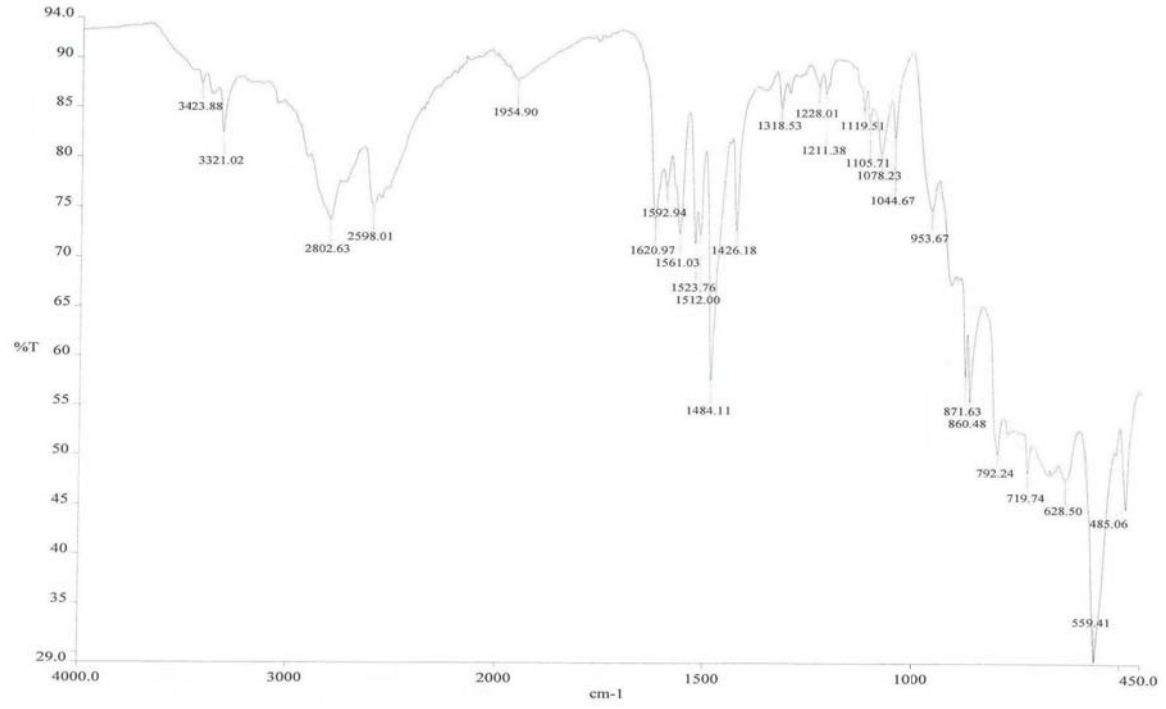

Figure B.7. FT-IR spectrum of $[MoO_2Cl_2((H_2N)C_6H_2Cl_2)]$ **(VII)**

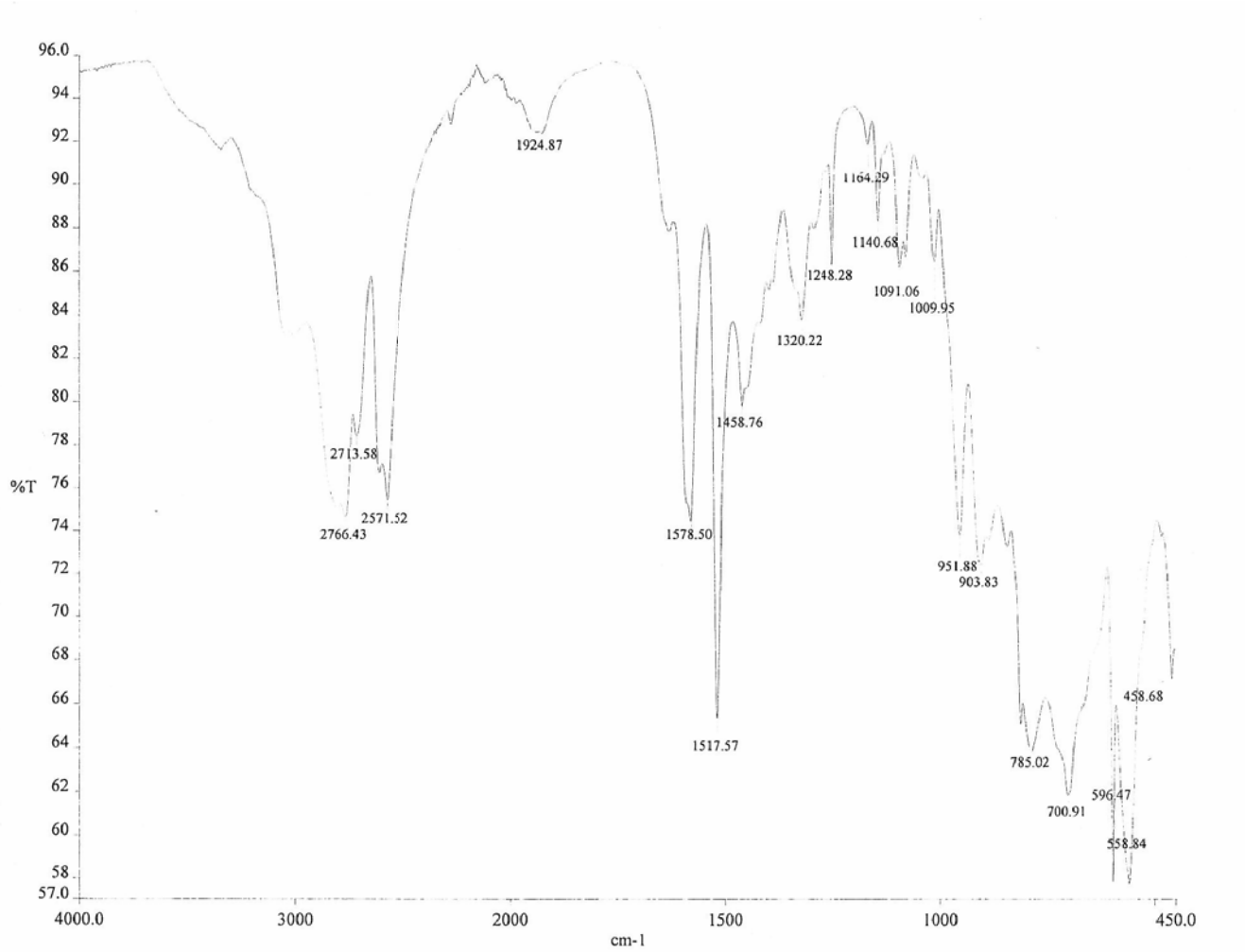

Figure B.8. FT-IR spectrum of $[MoO_2Cl_2(HNNH_2C_6(CH_3)_4)]$ **(VIII)**

APPENDIX C

CARTESIEN COORDINATES OF OPTIMIZED COMPLEXES

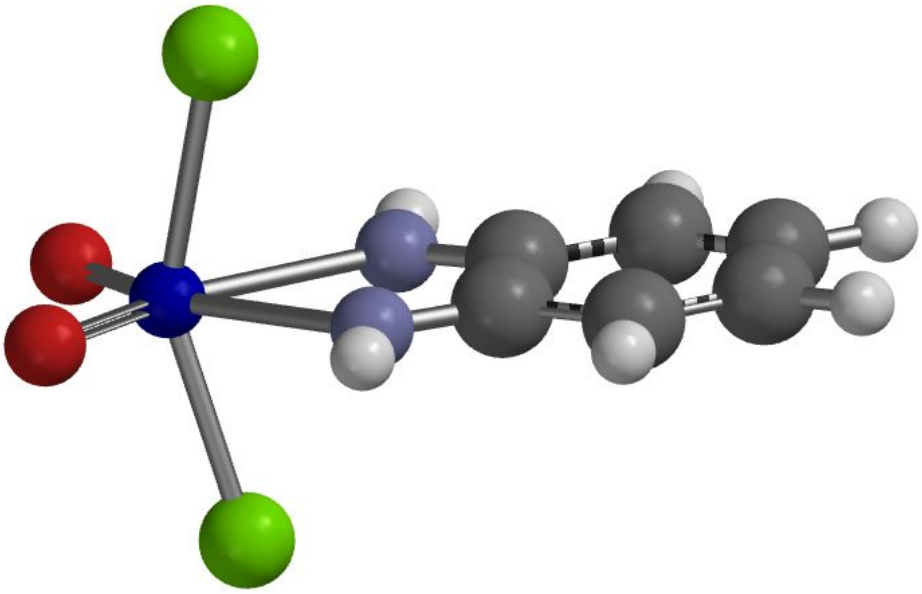

Figure C.1. DFT Calculated Complex $[MoO_2Cl_2((HN)_2C_6H_4)]$ **(I)**

Table C.1. Cartesian Coordinates of $[MoO_2Cl_2((HN)_2C_6H_4)]$ (I)

ATOM	X	Y	Z
Mo	0.00000000	0.00000000	-1.46122973
O	1.37400000	0.00000000	-2.47722973
O	-1.37400000	0.00000000	-2.47722973
Cl	0.00000000	-2.33900000	-0.89322973
Cl	0.00000000	2.33900000	-0.89322973
N	1.30500000	0.00000000	0.55477027
N	-1.30500000	0.00000000	0.55477027
C	0.75200000	0.00000000	1.71677027
C	-0.72800000	0.00000000	4.14577027
C	1.44100000	0.00000000	2.99577027
C	-0.75200000	0.00000000	1.71677027
C	-1.44100000	0.00000000	2.99577027
C	0.72800000	0.00000000	4.14577027
H	-2.32500000	0.00000000	0.55577027
H	2.32500000	0.00000000	0.55577027
H	-2.52700000	0.00000000	2.99777027
H	2.52700000	0.00000000	2.99777027
H	1.24100000	0.00000000	5.10177027
H	-1.24100000	0.00000000	5.10177027

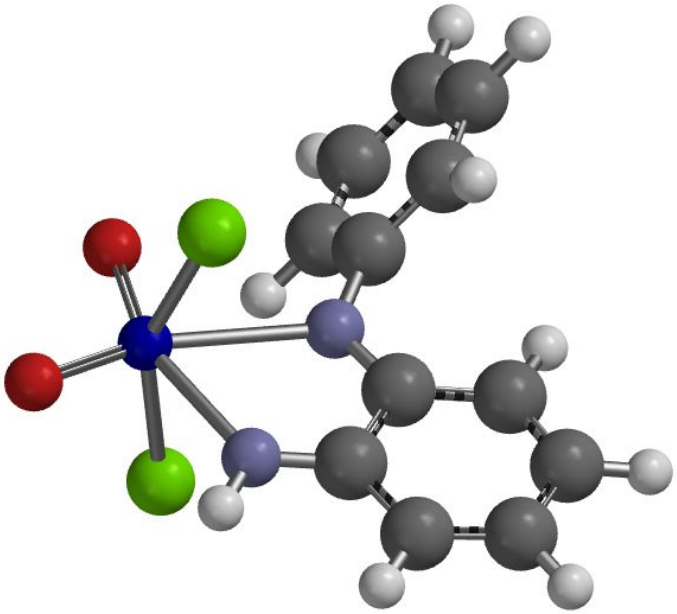

Figure C.2. DFT Calculated Complex $[MoO_2Cl_2((HN)(HNC_6H_5)C_6H_4)]$ **(II)**

Table C.2. Cartesian Coordinates of $[MoO_2Cl_2((HN)(HNC_6H_5)C_6H_4)]$ **(II)**

ATOM	X	Y	Z
Mo	1.45977660	-1.04487234	0.10486170
O	3.10777660	-1.43887234	0.29986170
O	0.59677660	-2.52087234	0.04986170
Cl	0.94777660	-0.47187234	2.38486170
Cl	1.46177660	-0.61287234	-2.26713830
N	1.80077660	1.25212766	0.07786170
N	-0.66622340	0.30312766	-0.13313830
C	0.85577660	2.12412766	-0.03013830
C	-1.34422340	3.89712766	-0.30113830
C	1.06177660	3.56012766	-0.03313830
C	-0.54322340	1.60012766	-0.13713830
C	-1.61622340	2.56912766	-0.28913830
C	0.00577660	4.40012766	-0.14913830
H	2.73977660	1.63812766	0.15086170
H	-2.62522340	2.20512766	-0.43413830
H	2.07777660	3.93212766	0.05786170
H	0.16377660	5.47412766	-0.15313830
H	-2.14822340	4.61112766	-0.44713830
C	-1.91922340	-0.34087234	-0.09913830
C	-4.35422340	-1.71087234	-0.03513830
C	-2.88822340	-0.01287234	0.86686170
C	-2.16022340	-1.38487234	-1.00813830
C	-3.38422340	-2.04487234	-0.98613830
C	-4.09622340	-0.70487234	0.89786170
H	-2.66422340	0.73912766	1.61586170
H	-1.39422340	-1.64587234	-1.72913830
H	-3.57622340	-2.83587234	-1.70413830
H	-4.83122340	-0.46387234	1.65886170
H	-5.29722340	-2.24687234	-0.01013830

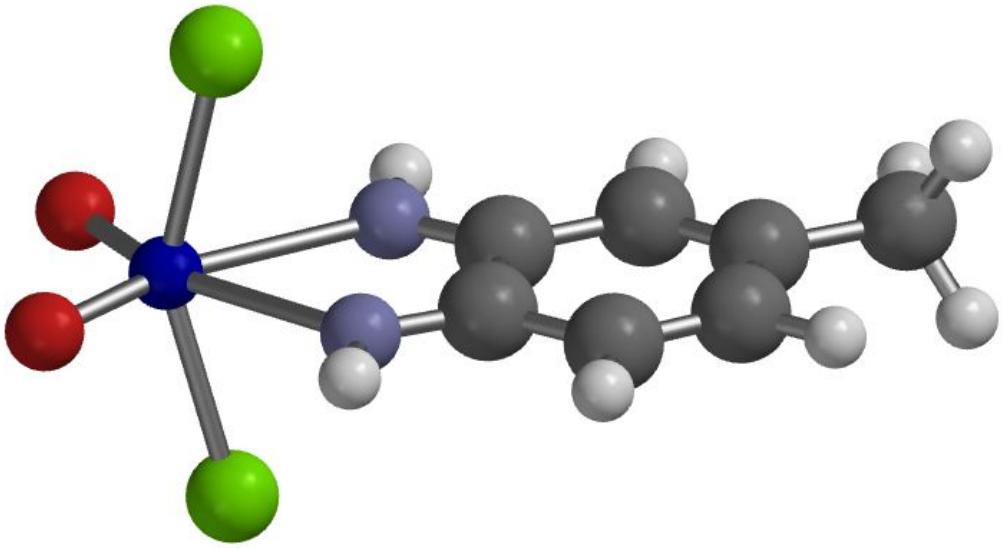

Figure C.3. DFT Calculated Complex $[MoO_2Cl_2((HN)_2C_6H_5(CH_3))]$ **(III)**

Table C.3. Cartesian Coordinates of $[MoO_2Cl_2((HN)_2C_6H_5(CH_3))]$ **(III)**

ATOM	X	Y	Z
Mo	-1.74923077	0.00018590	0.07588462
O	-2.87923077	-0.00581410	-1.20711538
O	-2.64323077	0.00718590	1.53088462
Cl	-1.18923077	-2.34181410	0.03188462
Cl	-1.19123077	2.34218590	0.01188462
N	0.14176923	-0.00581410	-1.40811538
N	0.36376923	0.00518590	1.19288462
C	1.34476923	-0.00381410	-0.95311538
C	3.90976923	0.00118590	0.33388462
C	2.56376923	-0.00581410	-1.74311538
C	1.47576923	0.00218590	0.54288462
C	2.80476923	0.00418590	1.12188462
C	3.76576923	-0.00381410	-1.12511538
C	5.30276923	0.00218590	0.89688462
H	0.45076923	0.00918590	2.20888462
H	0.05776923	-0.00981410	-2.42411538
H	2.88976923	0.00818590	2.20488462
H	2.48076923	-0.00981410	-2.82511538
H	4.67576923	-0.00481410	-1.71811538
H	5.85776923	-0.88081410	0.55788462
H	5.85976923	0.88018590	0.54688462
H	5.29976923	0.00918590	1.98888462

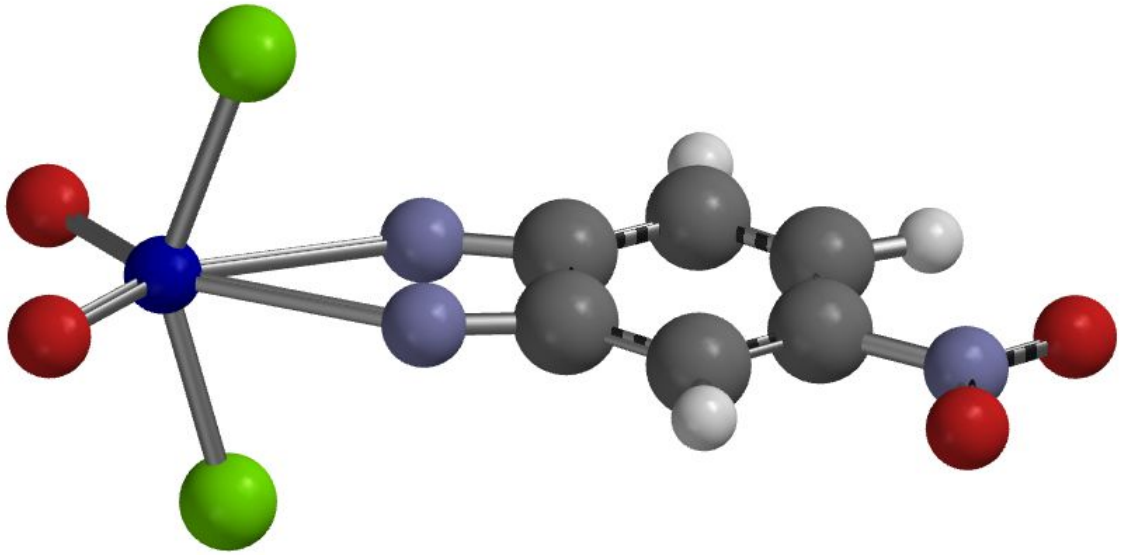

Figure C.4. DFT Calculated Complex [$MoO_2Cl_2(N_2C_6H_3(NO_2))$] **(IV)**

Table C.4. Cartesian Coordinates of $[MoO_2Cl_2(N_2C_6H_3(NO_2))]$ **(IV)**

ATOM	X	Y	Z
Mo	-2.42420238	0.11411905	0.00000000
O	-3.63120238	-1.07788095	0.00000000
O	-3.27720238	1.58011905	0.00000000
Cl	-1.74920238	0.03411905	2.27100000
Cl	-1.74920238	0.03411905	-2.27100000
N	-0.19620238	-1.06888095	0.00000000
N	0.03579762	0.65411905	0.00000000
C	1.10479762	-1.10488095	0.00000000
C	3.58879762	0.04211905	0.00000000
C	2.20579762	-2.03388095	0.00000000
C	1.29779762	0.33711905	0.00000000
C	2.59279762	0.96611905	0.00000000
C	3.41979762	-1.42488095	0.00000000
N	4.98879762	0.53811905	0.00000000
O	5.15679762	1.75211905	0.00000000
O	5.87979762	-0.30788095	0.00000000
H	4.33779762	-1.99988095	0.00000000
H	2.77979762	2.03211905	0.00000000
H	2.08879762	-3.11088095	0.00000000

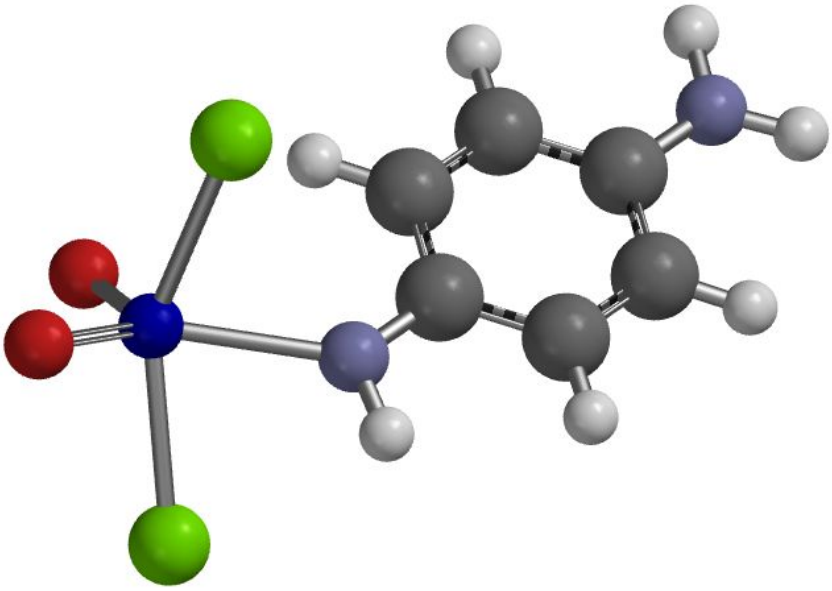

Figure C.5. DFT Calculated Complex $[MoO_2Cl_2((HN)_2C_6H_4)]$ **(V)**

Table C.5. Cartesian Coordinates of $[MoO_2Cl_2((HN)_2C_6H_4)]$ **(V)**

ATOM	X	Y	Z
Mo	-1.76193289	-0.17993960	0.12109396
O	-3.34593289	-0.52493960	-0.41990604
Cl	-2.17393289	2.18706040	0.22209396
Cl	-0.76393289	-2.04993960	-0.97290604
C	1.43306711	0.50606040	-0.33190604
C	4.17406711	-0.00293960	0.21609396
C	1.82906711	-0.50393960	0.60609396
C	2.47706711	1.26106040	-0.96490604
C	3.80006711	1.01306040	-0.70390604
C	3.15206711	-0.74493960	0.86909396
N	5.48406711	-0.25093960	0.47809396
O	-1.64193289	-0.62593960	1.76109396
N	0.14506711	0.74606040	-0.59990604
H	6.21406711	0.22506040	-0.02690604
H	5.75706711	-1.01193960	1.07909396
H	3.43006711	-1.51293960	1.58409396
H	1.06306711	-1.07693960	1.11509396
H	4.57206711	1.59206040	-1.20290604
H	2.20206711	2.03806040	-1.67290604
H	0.01306711	1.54406040	-1.21790604

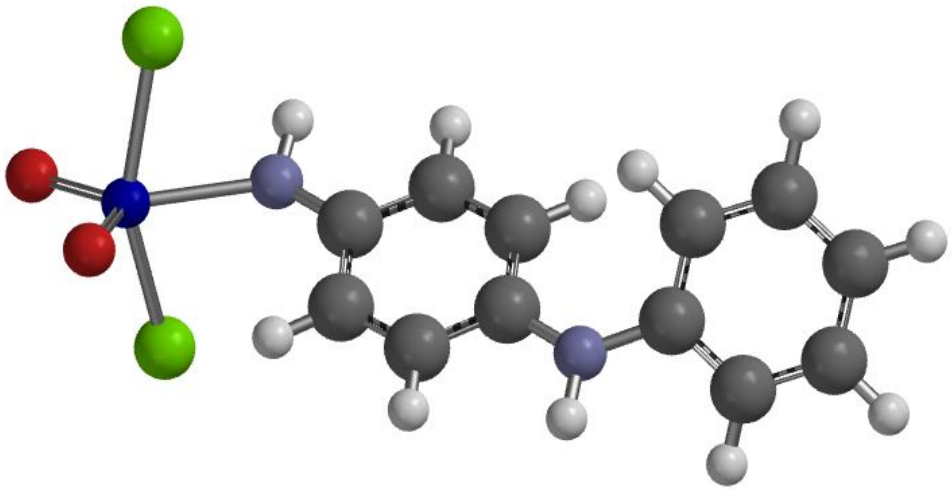

Figure C.6. DFT Calculated Complex $[MoO_2Cl_2((HN)(HNC_6H_5)C_6H_4)]$ **(VI)**

Table C.6. Cartesian Coordinates of $[MoO_2Cl_2((HN)(HNC_6H_5)C_6H_4)]$ **(VI)**

ATOM	X	Y	Z
Mo	-3.44892593	-0.00597354	-0.12312169
O	-3.45892593	0.42602646	-1.77212169
O	-5.05492593	-0.05797354	0.45287831
N	-1.49192593	-0.48497354	0.79687831
Cl	-3.25992593	-2.40897354	-0.30112169
Cl	-2.90592593	2.11402646	0.84487831
C	-0.24292593	-0.11797354	0.49987831
C	2.43007407	0.57202646	-0.19012169
C	0.88307407	-0.71697354	1.15587831
C	0.03307407	0.87702646	-0.49712169
C	1.32307407	1.20302646	-0.82212169
C	2.17307407	-0.38697354	0.82587831
N	3.69507407	0.94602646	-0.56512169
H	-0.79392593	1.36602646	-0.99912169
H	1.50907407	1.94702646	-1.59212169
H	2.99907407	-0.83997354	1.35987831
H	0.69807407	-1.44397354	1.94087831
H	3.75207407	1.78902646	-1.12012169
C	4.93407407	0.32702646	-0.28812169
C	7.44807407	-0.81597354	0.18487831
C	5.07107407	-1.06797354	-0.21612169
C	6.06607407	1.14302646	-0.14612169
C	7.31407407	0.57102646	0.08387831
C	6.32307407	-1.62697354	0.03187831
H	8.42007407	-1.25897354	0.37087831
H	8.18307407	1.21202646	0.19487831
H	5.96007407	2.22302646	-0.20312169
H	4.21207407	-1.70797354	-0.38212169
H	6.41907407	-2.70697354	0.08487831
H	-1.53092593	-1.24797354	1.46887831

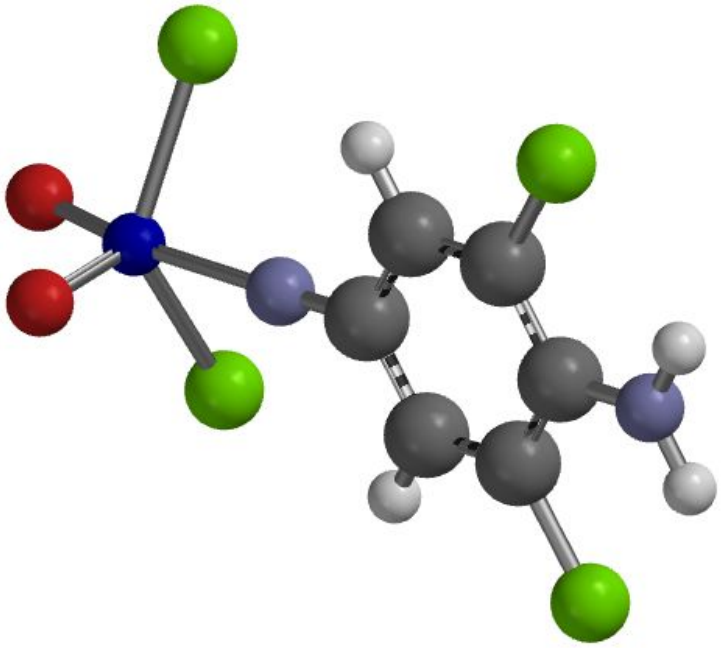

Figure C.7**.** DFT Calculated Complex $[MoO_2Cl_2((H_2N)C_6H_2Cl_2)]$ **(VII)**

Table C.7**.** Cartesian Coordinates of $[MoO_2Cl_2((H_2N)C_6H_2Cl_2)]$ **(VII)**

ATOM	X	Y	Z
Mo	-1.76193289	-0.17993960	0.12109396
O	-3.34593289	-0.52493960	-0.41990604
Cl	-2.17393289	2.18706040	0.22209396
Cl	-0.76393289	-2.04993960	-0.97290604
C	1.43306711	0.50606040	-0.33190604
C	4.17406711	-0.00293960	0.21609396
C	1.82906711	-0.50393960	0.60609396
C	2.47706711	1.26106040	-0.96490604
C	3.80006711	1.01306040	-0.70390604
C	3.15206711	-0.74493960	0.86909396
N	5.48406711	-0.25093960	0.47809396
O	-1.64193289	-0.62593960	1.76109396
N	0.14506711	0.74606040	-0.59990604
H	6.21406711	0.22506040	-0.02690604
H	5.75706711	-1.01193960	1.07909396
H	3.43006711	-1.51293960	1.58409396
H	1.06306711	-1.07693960	1.11509396
H	4.57206711	1.59206040	-1.20290604
H	2.20206711	2.03806040	-1.67290604
H	0.01306711	1.54406040	-1.21790604

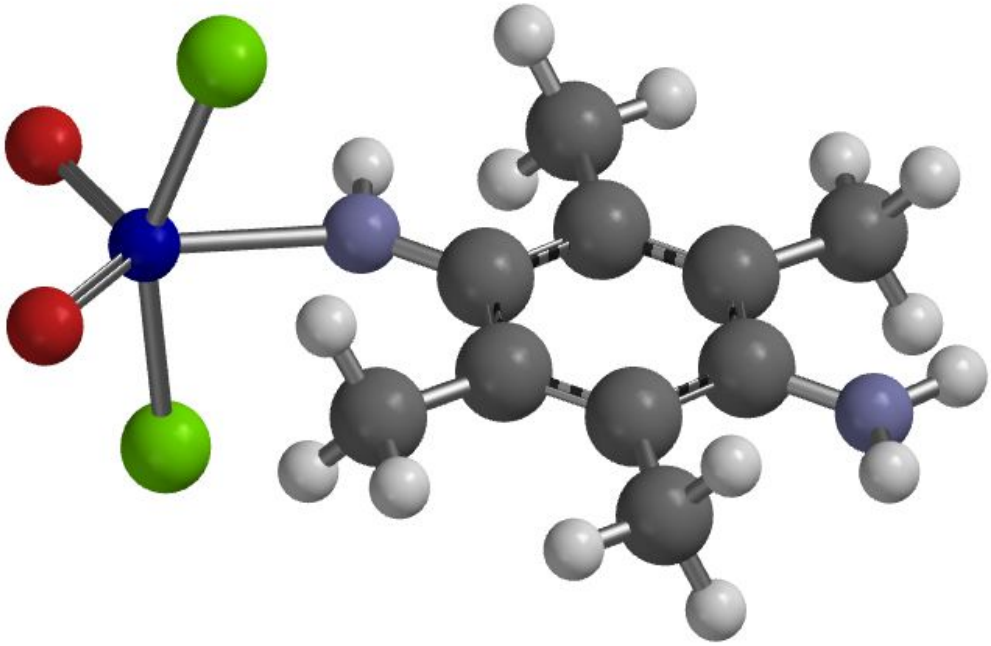

Figure C.8. DFT Calculated Complex $[MoO_2Cl_2(HNNH_2C_6(CH_3)_4)]$ **(VIII)**

Table C.8. Cartesian Coordinates of $[MoO_2Cl_2(HNNH_2C_6(CH_3)_4)]$ **(VIII)**

ATOM	X	Y	Z
Mo	2.34517127	-0.02906077	0.00608840
O	3.16517127	1.46893923	0.01708840
Cl	1.87817127	-0.01706077	-2.36591160
Cl	1.82417127	-0.01306077	2.36908840
C	-1.01082873	-0.38506077	-0.00991160
C	-3.69582873	0.38393923	-0.00091160
C	-1.35282873	1.02093923	-0.01091160
C	-2.05282873	-1.39706077	-0.00791160
C	-3.38182873	-1.01206077	-0.00591160
C	-2.68582873	1.39493923	-0.00691160
N	-5.00582873	0.76493923	-0.00391160
O	3.49517127	-1.28606077	0.02308840
N	0.27217127	-0.76406077	-0.01391160
H	-5.74582873	0.08893923	0.07108840
H	-5.25982873	1.73393923	0.07708840
H	0.36517127	-1.77706077	-0.02391160
C	-1.61282873	-2.84206077	-0.00591160
C	-4.54582873	-1.97706077	-0.00591160
C	-3.15682873	2.83193923	-0.01091160
C	-0.21782873	2.00693923	-0.01891160
H	-4.23782873	-3.01906077	-0.02491160
H	-5.18882873	-1.82106077	-0.88191160
H	-5.16782873	-1.84806077	0.89008840
H	-2.33882873	3.54693923	-0.03291160
H	-3.74982873	3.05893923	0.88608840
H	-3.78582873	3.03993923	-0.88591160
H	0.41117127	1.87493923	0.86808840
H	-0.54582873	3.04393923	-0.01691160
H	-1.02082873	-3.07706077	-0.89991160
H	-0.99382873	-3.06606077	0.87208840
H	-2.44582873	-3.54006077	0.01208840
H	0.40017127	1.87193923	-0.91191160